Networks and Heterogeneous Media

https://www.aimspress.com/journal/nhm

NHM, 19(3): 1085–1115.
DOI: 10.3934/nhm.2024048
Received: 15 July 2024
Revised: 13 September 2024
Accepted: 30 September 2024
Published: 09 October 2024

Research article

Higher-order convergence analysis for interior and boundary layers in a semi-linear reaction-diffusion system networked by a k-star graph with non-smooth source terms

Dilip Sarkar[1], Shridhar Kumar[1], Pratibhamoy Das[1] and Higinio Ramos[2,*]

[1] Department of Mathematics, Indian Institute of Technology Patna, Bihar 801106, India

[2] Department of Applied Mathematics, Universidad de Salamanca, Campus Viriato, Zamora 49022, Spain

* **Correspondence:** Email: higra@usal.es.

Abstract: We investigated a nonlinear singularly perturbed elliptic reaction-diffusion coupled system having non-smooth data networked by a k-star graph. We considered all possible boundary conditions at the free boundary located at the tail of the edge and imposed the continuity condition with Kirchhoff's junction law at the junction point of the k-star graph to obtain a continuous solution for this coupled system. First, we showed the existence and uniqueness of the solution using the variational formulation approach. Then, we reformulated it into a minimization problem over a function space to conclude the uniqueness of the solution. For the approximation of the continuous problem, note that the upwind scheme for the flux condition at the free boundary leads to a parameter uniform first-order approximation. To obtain a higher-order uniform accuracy, we utilized a three-point scheme for first-order derivatives and a five-point approximation at the point of discontinuity. These approximations typically did not yield an M-matrix or strict diagonally dominant structure of the stiffness matrix. Hence, we provided a suitable transformation that could lead to a sufficient condition for preserving the strict diagonally dominant structure of the stiffness matrix. We performed a comprehensive convergence analysis to demonstrate the almost second-order uniform accuracy on each edge of the k-star graph. Numerical experiments highly validate the theory on the k-star graph.

Keywords: k-star graph; minimization problem; optimization over function space; variational formulation; nonlinear reaction-diffusion problem; mixed boundary condition; singularly perturbed problem; non-smooth input data; higher-order accuracy

1. Introduction

Differential equations on connected graphs are an emerging research domain with several applications in physical, chemical, and biological models. In physical processes, such as lateral oscillations within a network of strings, beam vibrations connected by a network, and the stationary states of electrons within a molecule, the modeling has been done typically through boundary value problems on each edge of the network [1]. Pavlov et al. [2] gives a concrete example, where the free electrons encompass the interaction between molecules and their surrounding medium by a second-order boundary value problem connected by a graph. These problems are connected by a continuity condition at the junction nodes, which imposes the equilibrium of forces acting on each node from the adjacent edges. In [3], Nagatani formulates a traffic flow model on a star graph using a nonlinear diffusion equation. He examines traffic flow management by employing cell transmission on the graphs. The concept of discontinuity in traffic flow on each edge of the graph arises because the continuous flow may not be possible through the connecting vertices of the star, cycle, and complete graphs. It is important to note that a graph $\mathcal{G}$ is a finite set of vertices $V(\mathcal{G})$ connected by a finite set of edges $E(\mathcal{G})$ with a relation between each edge and corresponding two vertices (endpoints) (see [4]). More concrete applications on differential equations connected by a graph appear inside chemical models [5] where a neural network model predicts the chemical reactivity. One can also look into reaction-diffusion models in ecological and chemical contexts [6] and the blood flow model inside vessels in one-dimensional flow [7, 8].

Since graph theoretical models are different than usual problems, there are limited attempts to consider the existence of solutions for problems connected by the star graphs. In [9], the authors find the non-constant solution of the reaction-diffusion problem under the continuity and Kirchhoff conditions at the junction vertices. After that, Iwasaki et al. investigated the stability and instability of wave solutions of the reaction-diffusion problems on a metric graph in [10]. A theoretical approach to nonlinear fractional differential equations is also presented in [11] to demonstrate the well-posedness with Ulam Hyers stability. Existence and uniqueness results for fractional differential equations on a k-star graph domain are explored in [12]. The numerical approximation of differential equations connected by star graphs has received attention from a few authors. Gordezian et al. [13] considered a second-order linear differential equation on each edge of the k-star graph (see Figure 1) and used the Dirichlet boundary conditions at the outer vertices and the continuity preserving Kirchhoff's condition at the junction vertex. Their numerical analysis uses a central difference scheme for second-order derivatives and a forward difference scheme for first-order derivatives to achieve linear accuracy across the domain.

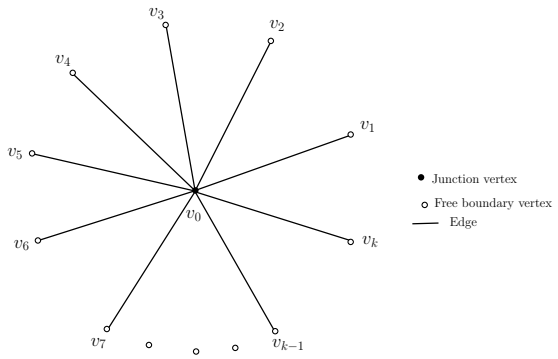

Figure 1. k- Star Graph ($\mathcal{G}$).

Singularly perturbed differential equations are crucial due to their extensive applications in hydrodynamics and gas dynamics. The concepts of boundary and interior layers in these areas were introduced in the nineteenth century. Ongoing efforts aim to understand the boundary and interior layer simulations associated with various singularly perturbed differential equations, including the viscous Burgers' and Navier–Stokes equations. For a recent survey that references singularly perturbed boundary value problems, one can refer to Gie [14]. In the present analysis, we focus on the effect of unbounded solution derivatives due to the presence of the viscosity parameter and show its complicacy to obtain the approximate solutions in maximum norm due to the presence of the viscosity parameter.

In [15], the authors provide a higher-order error analysis for the boundary layer-oriented singularly perturbed reaction-diffusion coupled systems with mixed boundary conditions on an equidistributed mesh. The nonlinear singularly perturbed problems and their coupled version are also considered for optimal convergence analysis in [16–20] on the equidistributed meshes. Note that the computational cost gradually increases with the number of equations in coupled systems. Therefore, the reduction of computational cost is also an important feature, which is carried out in [21–23] for reaction-dominated problems having different diffusion parameters. However, the generation of this mesh is relatively more complicated than the piecewise uniform meshes used in this article. Analogously, the problems on the k-star graph are also relatively complex and behave like a coupled system since edges are connected at a junction point. We refer to [24–26] for the well-posedness of the nonlinear hyperbolic conservation law on the network. Numerical approximation based on finite volume discretization for the hyperbolic conservation problem has been developed in [24, 27]. Moreover, validation of these schemes has been done in [28] by utilizing the exact solution of the Riemann problem.

Furthermore, the linear transport problem on the network has been considered for convergence analysis of the analytical solution based on parabolic approximation by utilizing the suitable transmission conditions in the inner node [29, 30]. For the numerical approximation, we refer to [31, 32], where the authors proposed a hybrid discontinuous Galerkin method to find the numerical solution on the network and provide the detailed analysis for the error estimate. Here, we are interested in the nonlinear singularly perturbed elliptic problem with non-smooth data on the star-shaped network for the convergence analysis of the higher-order scheme along with strong numerical evidence. However, some works are available on studying singular perturbation problems on the k-star graphs with smooth data. Kumar et al. [33] discuss a linear singularly perturbed reaction-diffusion problem connected by a star graph, with Dirichlet boundary conditions at the outer vertices, and the continuity and Kirchhoff's conditions at the junction point. This work utilizes a central difference scheme for the first and second-order derivatives over a piecewise uniform Shishkin mesh to obtain an almost second-order convergence. They consider the M-matrix criteria to derive the maximum principle based on the discretization of the graph Laplacian. However, it is unclear from the numerical point of view. Hence, there is a research gap on nonlinear singularly perturbed boundary value problems with non-smooth data, particularly in producing higher-order accurate uniformly stable solutions. In this regard, we mention the seminal monograph [34] having non-smooth source functions, which considers a linear singularly perturbed reaction-diffusion problem with Dirichlet boundary conditions on the fitted mesh to obtain parameter uniform linear accurate solutions. Moreover, a higher-order accuracy was obtained for convection-dominated problems having discontinuous convection terms to get an almost second-order accuracy based on a five-point scheme at the point of discontinuity [35]. One can also see more higher-order schemes [36, 37] to obtain uniformly convergent solutions in space. The increasing need for real-life issues such as flow

rate optimization [7, 8], reaction-dominated processes [33], and convection-dominated processes [38] drive the study of elliptic problems on networks. Elliptic partial differential equations (PDEs) describe equilibrium states where the system is balanced and no temporal changes occur. While studying these equations on networks, the solutions must account for the network's specific structure and satisfy the equilibrium conditions at each node to ensure continuity and compatibility across the network's junction points. These complexities are not typically encountered while studying scalar elliptic problems defined on simple domains [34]. Therefore, we study a more general class of elliptic problems with non-smooth source terms, which are typically applicable in real-world scenarios.

Based on the above motivations, we observe that nonlinear steady-state singularly perturbed reaction-diffusion problems having discontinuous source terms with mixed boundary conditions are more general and realistic from applied sciences on a star graph domain. Our major goals are the higher-order accurate results for this class of problems and their mathematical analysis with numerical difficulties.

The structure of this paper is as follows: In Section 2, we state a nonlinear reaction-diffusion problem with non-smooth data on a k-star graph. In Section 3, we analyze the properties of the analytic solution and provide its derivative bounds. In Section 4, we present a discretization using a three-point scheme and a five-point scheme on the Shishkin mesh on the k-star graph. We also estimate the maximum error within the graph domain. In Section 5, we focus on the numerical experiments conducted on the 3-star graph, investigate its errors, and analyze the convergence of experimental results of the test problem.

2. Problem description

A k-star graph $\mathcal{G}$ is a collection of a finite set of vertices $V(\mathcal{G}) = \{v_i;\ i = 0, 1, \cdots, k\}$, and edges $E(\mathcal{G}) = \{e_i;\ i = 1, \cdots, k\}$, where all the k vertices $v_i's$ for $i = 1, \cdots, k$ (see Figure 1) have degree (no. of edges incident on that vertex) 1, and one central vertex (see, v_0 in Figure 1) has degree k (v_0 is incident with k edges). Here v_0 is called the junction point, and e_i defines the edge joining the vertex v_i to the junction vertex v_0, i.e., $e_i = \overrightarrow{v_i v_0}$. We also consider $\ell_i = |e_i| = |\overrightarrow{v_i v_0}|$, for all $i = 1, \cdots, k$. Then, the singularly perturbed boundary layer-originated problems are defined on each edge of the k-star graph $\mathcal{G}$ and connected at the junction point.

Hence, without loss of generality, we assume each outer vertex v_i, for $i = 1, \cdots, k$, as an origin. We can identify each edge e_i as $e_i := (0, \ell_i)$. Then, the singularly perturbed semi-linear reaction-diffusion problem with discontinuous source term as given on the k-star graph, where we represent u along the ith edge u_i, is defined by:

$$T_{\varepsilon_i} u_i(x) := -\varepsilon_i u_i''(x) + f_i(x, u_i(x)) = g_i(x), \quad \text{on} \quad x \in \Omega_i^- \cup \Omega_i^+, \quad i = 1, 2, \cdots, k, \tag{2.1}$$

$$T_{0_i} u_i(0) := -\mu_{i,1} u_i(0) + \mu_{i,2} u_i'(0) = \psi_i, \ i = 1, 2, \cdots, k, \tag{2.2}$$

$$T_{\ell_i} u_i(\ell_i) = T_{\ell_m} u_m(\ell_m) := u^J \text{ (Continuity condition)}, \ i \neq m, \text{ and } i, m = 1, 2, \cdots, k, \tag{2.3}$$

$$\sum_{i=1}^{k} \varepsilon_i u_i'(\ell_i) = 0 \text{ (Kirchoff's Junction Law)}, \tag{2.4}$$

where T_{ε_i} is a nonlinear operator, defined by $T_{\varepsilon_i} u_i(x) := -\varepsilon_i u_i''(x) + f_i(x, u_i(x))$, T_{0_i} is the linear operator at the free boundary vertices, defined by $T_{0_i} u_i(0) := -\mu_{i,1} u_i(0) + \mu_{i,2} u_i'(0)$ and $T_{\ell_i} \equiv I$ is the identity operator, defined by $T_{\ell_i} u_i(\ell_i) := u_i(\ell_i)$ and, u^J is unknown where the superscript J indicates the junction point, $\Omega_i^- = (0, d_i)$, $\Omega_i^+ = (d_i, \ell_i)$ and $\Omega_i = \Omega_i^- \cup \Omega_i^+$. We assume that source term $g_i(x)$ is discontinuous

at the point $x = d_i$, i.e., $g_i(d_i-) \neq g_i(d_i+)$, where $d_i \in e_i = (0, \ell_i)$. We also assume that ψ_i, $\mu_{i,1}$ are positive constants and $\mu_{i,2}$ is either a constant or takes the value ε_i. The jump of any function δ at d_i is denoted by $[\delta](d_i) = \delta(d_i+) - \delta(d_i-)$. For all $x \in \bar{\Omega}_i$, we assume that the semi-linear term $f_i(x, u_i(x))$ is sufficiently smooth, $f_i(x, 0) = 0$ and satisfy the following condition

$$\delta_i^* \geq \frac{\partial f_i(x, u_i(x))}{\partial u_i} \geq \delta_i > 0, \text{ for some positive constants } \delta_i \text{ and } \delta_i^*. \tag{2.5}$$

Note that $u_i(x) \notin C^2(e_i)$, as g_i is discontinuous at d_i, and $u_i(d_i+) = u_i(d_i-)$.

The reduced problem corresponding to Eqs (2.1)–(2.4) is defined by

$$f_i(x, u_i^0(x)) = g_i(x), \text{ on } \Omega_i. \tag{2.6}$$

Since the source term $g_i(x)$ is discontinuous at the point $x = d_i$, we expect an interior layer of width $O(\sqrt{\varepsilon})$ near the discontinuity point [34].

Notation: In this paper, C denotes a generic positive constant independent of the diffusion parameters ε_i and the number of step sizes N_i. Here, $\frac{\partial f}{\partial u}(x, .)$ denotes the partial derivative concerning the dependent variable. $\|\cdot\|_{\Omega^N}$ denotes the maximum norm over a given mesh function on the domain Ω^N. We use the symbol $C^p(\Omega)$ to represent the space of p-th time continuously differentiable functions on the domain Ω.

3. Analytical properties

In this section, we discuss the analytical behavior of the solution on each edge of the k-star graph domain. Let us assume $e_i = (0, \ell_i) = (0, 1)$, on every edge of the k-star graph, for all $i = 1, 2, \cdots, k$.

Theorem 1. *On each edge of the k-star graph domain, let u_i be the solution of the ith edge for $1 \leq i \leq k$. Then $u_i \in C^0(\bar{e}_i) \cap C^1(e_i) \cap C^2(\Omega_i^- \cup \Omega_i^+)$.*

Proof. Let u_i be the solution of the ith edge, and $u_{i,1}$ and $u_{i,2}$ be the particular solutions of the following nonlinear differential equations

$$-\varepsilon_i u_{i,1}''(x) + f_i(x, u_{i,1}(x)) = g_i(x), \ x \in \Omega_i^-, \quad \text{and} \quad -\varepsilon_i u_{i,2}''(x) + f_i(x, u_{i,2}(x)) = g_i(x), \ x \in \Omega_i^+,$$

where $u_{i,1} \in C^2(\Omega_i^-)$ and $u_{i,2} \in C^2(\Omega_i^+)$.
Consider the function

$$u_i = \begin{cases} u_{i,1}(x) + \left(\psi_i - T_{0_i} u_{i,1}(0)\right) \Upsilon_{i,1}(x) + A\Upsilon_{i,2}(x), & x \in \Omega_i^-, \\ u_{i,2}(x) + B\Upsilon_{i,1}(x) + \left(u^J - u_{i,2}(1)\right) \Upsilon_{i,2}(x), & x \in \Omega_i^+, \end{cases} \tag{3.1}$$

where $\Upsilon_{i,1}$ and $\Upsilon_{i,2}$ are defined as follows

$$-\varepsilon_i \Upsilon_{i,1}''(x) + f_i\left(x, \Upsilon_{i,1}(x)\right) = 0, \ \ \Upsilon_{i,1}(0) = 1, \ \Upsilon_{i,1}(1) = 0, \text{ on } x \in e_i, \tag{3.2}$$

$$-\varepsilon_i \Upsilon_{i,2}''(x) + f_i\left(x, \Upsilon_{i,2}(x)\right) = 0, \ \Upsilon_{i,2}(0) = 0, \ \Upsilon_{i,2}(1) = 1, \text{ on } x \in e_i. \tag{3.3}$$

Here, we choose the constants A and B in such a way that $u_i \in C^1(e_i)$ and $u_i \in C^2(\Omega_i^- \cup \Omega_i^+)$. Note that the solutions of Eqs (3.2) and (3.3) on $(0, 1)$, $0 < \Upsilon_{i,1}, \Upsilon_{i,2} < 1$,. Thus, we cannot have maximum and minimum in the interior points, and hence $\Upsilon_{i,1}' < 0, \ \ \Upsilon_{i,2}' > 0$ on the interval $(0, 1)$.

Now, we choose the constants A and B by imposing the following condition, which ensures the continuous differentiability at all the interior points, i.e., $u_i \in C^1(e_i)$. Based on this, we can write

$$u_i(d_i-) = u_i(d_i+), \quad \text{and} \quad u_i'(d_i-) = u_i'(d_i+).$$

From the above conditions, we get

$$\begin{aligned} A\Upsilon_{i,2}(d_i) - B\Upsilon_{i,1}(d_i) &= (u^J - u_{i,2}(1))\Upsilon_{i,2}(d_i) - (\psi_i - T_{0_i}u_{i,1}(0))\,\Upsilon_{i,1}(d_i), \\ A\Upsilon'_{i,2}(d_i) - B\Upsilon'_{i,1}(d_i) &= (u^J - u_{i,2}(1))\Upsilon'_{i,2}(d_i) - (\psi_i - T_{0_i}u_{i,1}(0))\,\Upsilon'_{i,1}(d_i). \end{aligned}$$

For the existence of A and B, we need

$$\begin{vmatrix} \Upsilon_{i,2}(d_i) & -\Upsilon_{i,1}(d_i) \\ \Upsilon'_{i,2}(d_i) & -\Upsilon'_{i,1}(d_i) \end{vmatrix} \neq 0.$$

This gives $\Upsilon'_{i,2}(d_i)\Upsilon_{i,1}(d_i) - \Upsilon'_{i,1}(d_i)\Upsilon_{i,2}(d_i) \neq 0$. Hence, $u_i \in C^0(\bar{e}_i) \cap C^1(e_i) \cap C^2(\Omega_i^- \cup \Omega_i^+)$ exists.

The well-posedness of the problem is considered in the Hilbert space framework. From Eq (2.1) along with the homogeneous boundary conditions (2.2)–(2.4) (by assuming $\psi_i = 0$ and $u^J = 0$) on ith edge e_i, we define the pivotal space of the entire graph $\mathcal{G}$ as

$$H(\mathcal{G}) := L^2(\mathcal{G}) := \prod_{i=1}^{k} L^2(0,\ell_i) = \Big\{u;\, u|_{e_i} = u_i,\ u_i \in L^2(0,\ell_i),\ \text{for all } i = 1,\cdots,k\Big\}.$$

Now, we define the Sobolev space on e_i:

$$H^1_{e_i} := \Big\{u_i \in L^2(e_i); u_i' \in L^2(e_i) \text{ for all } i\Big\},$$

and, the Sobolev space on the graph $\mathcal{G}$

$$H^1(\mathcal{G}) = \Big\{u \in L^2(\mathcal{G});\ u|_{e_i} = u_i, \text{ and } u_i \in H^1_{e_i} \text{ for all } e_i \in E(\mathcal{G})\Big\}.$$

Define the corresponding Sobolev norm [30] as follows:

$$\|\eta\|^2_{L^2(\mathcal{G})} = \sum_{e_i \in E(\mathcal{G})} \|\eta_i\|^2_{L^2(e_i)}, \quad \text{and} \quad (\eta,\lambda)_{L^2(\mathcal{G})} = \sum_{e_i \in E(\mathcal{G})} (\eta_i,\lambda_i)_{L^2(e_i)}.$$

Similarly,

$$\|\eta\|^2_{H^1(\mathcal{G})} = \sum_{e_i \in E(\mathcal{G})} \|\eta_i\|^2_{H^1(e_i)} \quad \text{and} \quad (\eta,\lambda)_{H^1(\mathcal{G})} = \sum_{e_i \in E(\mathcal{G})} (\eta_i,\lambda_i)_{H^1(e_i)}.$$

Analogously, let us define the space on the edge e_i as $\mathbb{V}_i^* = \Big\{u_i \in H^1_{e_i}; T_{0_i}u_i(0) = 0\Big\}$, and introduce the dense space $\mathbb{D}^*(T_{\varepsilon_i}) := \Big\{u_i \in \mathbb{V}_i^*; T_{\varepsilon_i}u_i \in L^2(e_i)\Big\}$. Let us also define the spaces of the entire graph as $\mathbb{V}^* := \Big\{u \in H^1(\mathcal{G}); T_{\ell_i}u_i(\ell_i) = T_{\ell_k}u_k(\ell_k),\ \text{for all } i,k,\ \text{and } T_{0_i}u_i(0) = 0\Big\}$ and define the dense space on the entire graph $\mathcal{G}$ is $\mathbb{D}^*(L) := \Big\{u \in \mathbb{V}^*; u \in \prod_{i=1}^k \mathbb{D}^*(T_{\varepsilon_i}),\ \sum_{i=1}^k \varepsilon_i u_i'(\ell_i) = 0\Big\}$ on which we define the operator L as

$$L : \mathbb{D}^*(L) \subset H(\mathcal{G}) \longrightarrow H(\mathcal{G}), \quad Lu|_{e_i} := T_{\varepsilon_i}u_i.$$

Consider that $g \in H(\mathcal{G})$ such that $g|_{e_i} = g_i$. Multiplying the state equation (2.1) by an arbitrary test function $v \in \mathbb{D}^*(L)$ and integrating by parts, we get the weak formulation of the problems (2.1)–(2.4):

$$u \in \mathbb{D}^*(L), \quad B(u, v) = \langle g, v\rangle \quad \text{for all} \quad v \in \mathbb{D}^*(L). \tag{3.4}$$

Here, the quadratic form $B(\cdot,\cdot) : \mathbb{D}^*(L) \times \mathbb{D}^*(L) \longrightarrow \mathbb{R}$ is defined by

$$B(u, v) := \sum_{i=1}^{k} a_i(u_i, v_i) = \sum_{i=1}^{k} \int_{e_i} (\varepsilon_i u_i' v_i' + f_i(x, u_i)v_i)\, dx, \tag{3.5}$$

and

$$\langle g, v\rangle = \sum_{i=1}^{k} \int_{\Omega_i^- \cup \Omega_i^+} g_i v_i dx = \sum_{i=1}^{k} \left(\int_0^{d_i} g_i v_i + \int_{d_i}^{\ell_i} g_i v_i \right) dx. \tag{3.6}$$

Now, we introduce the minimization problem corresponding to the weak formulation (3.4)

$$u \in \mathbb{D}^*(L), \quad \mathbb{E}(u) = \inf_{v \in \mathbb{D}^*(L)} \mathbb{E}(v), \tag{3.7}$$

where

$$\mathbb{E}(v) = \sum_{i=1}^{k} \int_{e_i} \left(\frac{\varepsilon_i}{2} |v_i'|^2 + F_i(x, v_i) \right) dx - \sum_{i=1}^{k} \int_{\Omega_i^- \cup \Omega_i^+} g_i v_i dx, \tag{3.8}$$

is the "energy functional" and $F_i(x, v_i) = \displaystyle\int_0^{v_i} f_i(x, s)ds$.

Lemma 1. *The energy function $\mathbb{E}(\cdot)$ is coercive, continuous, strictly convex, Fréchet differentiable and it satisfies*

$$\langle \mathbb{E}'(u), v\rangle = \sum_{i=1}^{k} \int_{e_i} (\varepsilon_i u_i' v_i' + f_i(x, u_i)v_i)\, dx - \sum_{i=1}^{k} \int_{\Omega_i^- \cup \Omega_i^+} g_i v_i dx.$$

Proof. The result follows from [39, 40]. The rigorous procedure can be seen in [41].

Theorem 2. *Assume that $g \in H(\mathcal{G})$. Then, the weak formulation* (3.4) *and the minimization problem* (3.7) *are equivalent, and both admit a unique solution.*

Proof. The results follow from Lemma 1 by considering the analysis given in [40, 41].

Moreover, considering the velocity vector zero in the convection-diffusion-reaction nonlinear problem given in [42], the stability of the solution of the current nonlinear reaction-diffusion problem follows for $f_i(x, u_i(x)) = k_i(u_i)u_i$, where $k_i(u_i)$ satisfies the Lipschitz condition with respect to u_i. Note that we consider the test function $v = 0$ at the boundary.

3.1. Bounds of solution and its derivatives

For singularly perturbed reaction-diffusion problems, it is well known that the solution can have boundary and interior layers in its domain of definition depending on the smoothness of the data and boundary conditions. In these layer regions, the solution varies abruptly and has large, steep gradients. In contrast, outside these regions, the solution varies smoothly and has bounded derivatives up to some

finite order. A rigorous convergence analysis of numerical approximations; requires derivatives of the solution.

Hence, to simplify this convergence analysis, we decompose the solution into the regular component r_i and the singular component s_i such that $u_i = r_i + s_i$, on each ith edge of the graph. The regular component r_i, typically represents the smooth, well-behaved part of the solution that varies gradually across the domain and has bounded derivatives up to some finite order. This part is often associated with the domain's bulk or interior regions with minimal perturbation parameter effects. The convergence analysis for this component becomes more straightforward as the required derivatives for this analysis are bounded. The singular component s_i captures the rapid variations and steep gradients near boundaries or interfaces. In reaction-diffusion problems, these regions often exhibit behaviors not captured by the regular part alone, such as boundary or interior layers where the solution changes abruptly. The singular component s_i corrects the discrepancies between the regular part and the actual solution, especially near regions where the perturbation parameter has a significant impact. The analysis of this component is complicated, in general.

Let us assume $\mu_{i,2}$ is a constant. Therefore, we decompose the solution into two parts on each ith edge of the k-star graph domain, such that

$$u_i(x) = r_i(x) + s_i(x),$$

where $u_i(x)$ is a solution of the ith edge of the k-star graph domain.

Then, the regular component $r_i(x)$ satisfies the following problem

$$T_{\varepsilon_i} r_i(x) := -\varepsilon_i r_i''(x) + f_i(x, r_i(x)) = g_i, x \in \Omega_i^-,\ T_{0_i} r_i(0) = T_{0_i} u_i^0(0),\ T_{1_i} r_i(d_i-) = T_{1_i} u_i^0(d_i-), \quad (3.9)$$

$$T_{\varepsilon_i} r_i(x) := -\varepsilon_i r_i''(x) + f_i(x, r_i(x)) = g_i, x \in \Omega_i^+,\ T_{0_i} r_i(d_i+) = T_{0_i} u_i^0(d_i+),\ T_{1_i} r_i(1) = T_{1_i} u_i^0(1). \quad (3.10)$$

We further decompose the regular component solution r_i of Eq (3.9) into two different parts of the domain, so that the analysis available for problems having two boundary layers can be utilized in both the part of the domains separately. This decomposition is done as follows $r_i = v_{i,1} + v_{i,2}$, where $v_{i,1}$ is the solution of the following problem

$$\begin{aligned} &-\varepsilon_i v_{i,1}'' + f_i(x, v_{i,1}(x)) = 0, \quad x \in \Omega_i^- \\ &T_{0_i} v_{i,1}(0) = T_{0_i} r_i(0),\ T_{1_i} v_{i,1}(d_i-) = T_{1_i} r_i(d_i-), \end{aligned} \quad (3.11)$$

and $v_{i,2}$ is the solution of the following problem

$$\begin{aligned} &-\varepsilon_i v_{i,2}'' + f_i(x, (v_{i,2} + v_{i,1})(x)) - f_i(x, v_{i,1}(x)) = g_i(x), \quad x \in \Omega_i^- \\ &T_{0_i} v_{i,2}(0) = 0,\ T_{1_i} v_{i,2}(d_i-) = 0. \end{aligned} \quad (3.12)$$

Similarly, we can derive a similar expression from Eq (3.10) on the domain Ω_i^+.

Note that the singular component $s_i(x)$ satisfies the following problem

$$T_{\varepsilon_i} s_i(x) := -\varepsilon_i s_i'' + f_i(x, (r_i + s_i)(x) - f_i(x, r_i(x)) = 0, x \in \Omega_i^- \cup \Omega_i^+,$$

$$T_{0_i} s_i(0) = T_{0_i}(u_i - r_i)(0), \quad T_{1_i} s(1) = T_{1_i}(u_i - r_i)(1),$$

$$[s_i](d_i) = -[r_i](d_i), \quad [s_i'](d_i) = [r_i'](d_i).$$

Furthermore, we decompose the singular component $s_i(x)$, as follows

$$s_i(x) = \begin{cases} s_{L_i}(x), & x \in \Omega_i^-, \\ s_{R_i}(x), & x \in \Omega_i^+, \end{cases}$$

i.e., $s_{L_i}(x)$ is defined on Ω_i^- and $s_{R_i}(x)$ is defined on Ω_i^+. Then, from Theorem 1, singular component s_i is well defined; as follows

$$s_i = \begin{cases} T_{0_i} s_i(0)\phi_{i,1}(x) + \beta_1 \phi_{i,2}(x), & \text{for } x \in \Omega_i^-, \\ \beta_2 \phi_{i,3}(x) + T_{1_i} s_i(1)\phi_{i,4}(x), & \text{for } x \in \Omega_i^+, \end{cases}$$

where $\phi_{i,m}$ for $m = 1, 2, 3, 4$, satisfy the following boundary value problems

$$\begin{aligned}
&-\varepsilon_i \phi_{i,1}''(x) + f_i(x, s_i + \phi_{i,1}) - f_i(x, s_i) = 0, \ x \in \Omega_i^-, \ \ T_{0_i}\phi_{i,1}(0) = 1, \ \ T_{1_i}\phi_{i,1}(d_i) = 0, \\
&-\varepsilon_i \phi_{i,2}''(x) + f_i(x, s_i + \phi_{i,1} + \phi_{i,2}) - f_i(x, s + \phi_{i,1}) = 0, \ \ x \in \Omega_i^-, \ \ T_{0_i}\phi_{i,2}(0) = 0, \ \ T_{1_i}\phi_{i,2}(d_i) = 1, \\
&-\varepsilon_i \phi_{i,3}''(x) + f_i(x, s_i + \phi_{i,3}) - f_i(x, s_i) = 0, \ \ x \in \Omega_i^+, \ \ T_{0_i}\phi_{i,3}(d_i) = 1, \ \ T_{1_i}\phi_{i,3}(1) = 0, \\
&-\varepsilon_i \phi_{i,4}''(x) + f_i(x, s_i + \phi_{i,3} + \phi_{i,4}) - f_i(x, s_i + \phi_{i,3}) = 0, \ \ x \in \Omega_i^+, \ \ T_{0_i}\phi_{i,4}(d_i) = 0, \ \ T_{1_i}\phi_{i,4}(1) = 1,
\end{aligned}$$

and β_1 and β_2 are constants that we need to choose in such a way that the jump condition at $x = d_i$ is satisfied, that is,

$$\begin{aligned}
&T_{\varepsilon_i} s_{L_i}(x) = 0, \text{ on } \Omega_i^-, \\
&T_{0_i} s_{L_i}(0) = T_{0_i} s_i(0), \ T_{1_i} s_{L_i}(d_i-) = T_{1_i} s_i(d_i-),
\end{aligned} \tag{3.13}$$

and

$$\begin{aligned}
&T_{\varepsilon_i} s_{R_i}(x) = 0 \text{ on } \Omega_i^+, \\
&T_{0_i} s_{R_i}(d_i+) = T_{0_i} s_i(d_i+), \ T_{1_i} s_{R_i}(1) = T_{1_i} s_i(1).
\end{aligned} \tag{3.14}$$

From above, we can write

$$-\varepsilon_i s_{L_i}''(x) + b_i^1(x) s_{L_i}(x) = 0, \quad \text{on } \Omega_i^-, \tag{3.15}$$

where $b_i^1(x) = \displaystyle\int_0^1 \frac{\partial f_i}{\partial u_i}(x, r_i + q s_{L_i})dq$, and

$$-\varepsilon_i s_{R_i}''(x) + b_i^2(x) s_{R_i}(x) = 0, \quad \text{on } \Omega_i^+, \tag{3.16}$$

where $b_i^2(x) = \displaystyle\int_0^1 \frac{\partial f_i}{\partial u_i}(x, r_i + t s_{R_i})dt$.

Let us use the following notations for the layer functions

$$\Pi_1(x) = e^{-x\sqrt{\delta_i/\varepsilon_i}} + e^{-(d_i - x)\sqrt{\delta_i/\varepsilon_i}} \ \text{ and } \ \Pi_2(x) = e^{-(x-d_i)\sqrt{\delta_i/\varepsilon_i}} + e^{-(1-x)\sqrt{\delta_i/\varepsilon_i}}.$$

Theorem 3. *On the ith edge of the k-star graph domain, the regular component satisfies the following derivatives bounds*

$$\left|r_i^{(m)}(x)\right| \leq C, \;\; m = 0, 1, 2, 3, \qquad \left|r_i^{(4)}(x)\right| \leq C\, \varepsilon_i^{-1/2}, \quad \text{for } x \in e_i,$$

where C is independent of ε_i.

Proof. We can prove this theorem step by step. First, we establish the derivative bounds for the regular component on the domain Ω_i^- using Eqs (3.9), (3.11) and (3.12). We employ a similar argument as in Theorem 1; given in [43] to establish the bounds for the regular components and their derivatives. In a similar way, we can establish the derivative bounds of the regular components on Ω_i^+ using an analogous decomposition of the regular component from Eq (3.10) on the domain Ω_i^+. Finally, we obtain the bounds of the regular component and its derivatives by adding them over e_i.

Theorem 4. *On the ith edge of the k-star graph domain, the singular component satisfies the following bounds*

$$\begin{aligned}
&\left|s_{L_i}^{(m)}(x)\right| \leq C\, \Pi_1(x), \quad m = 0, 1\\
&\left|s_{L_i}^{(m)}(x)\right| \leq C\varepsilon_i^{-(m-1)/2}\, \Pi_1(x), \quad m = 2, 3, 4,\\
&\left|s_{R_i}^{(m)}(x)\right| \leq C\, \Pi_2(x), \quad m = 0, 1\\
&\left|s_{R_i}^{(m)}(x)\right| \leq C\varepsilon_i^{-(m-1)/2}\, \Pi_2(x), \quad m = 2, 3, 4, \quad x \in e_i,
\end{aligned}$$

where C is independent of ε_i.

Proof. The linear problems (3.15) and (3.16) together with the boundary conditions in Eqs (3.13) and (3.14) are similar to the problems considered in [43]. Hence, we obtain the bounds for s_{L_i} and s_{R_i} and their derivatives analogously.

Remark 1. *Consider that* $\mu_{i,2} = \varepsilon_i$. *In this case, the derivative bounds of the components will be sharp; compared to* $\mu_{i,2}$ *as a constant. Therefore, the bounds for Dirichlet type problems; will be used for further analysis, which is as follows*

$$\left|r_i^{(m)}(x)\right| \leq C(1 + \varepsilon_i^{-(m-2)/2}), \;\; m = 0, 1, 2, 3, 4, \text{ for } x \in e_i,$$

and

$$\left|s_i^{(m)}(x)\right| \leq \begin{cases} C\varepsilon_i^{-m/2}\Pi_1(x), & x \in \Omega_i^-, \\ C\varepsilon_i^{-m/2}\Pi_2(x), & x \in \Omega_i^+, \end{cases} \quad \text{for } m = 0, 1, 2, 3, 4.$$

4. Discretization and convergence analysis

Assume that $e_i = (0, 1)$ which is obtained by setting $\ell_i = 1$, for all $i = 1, 2, \cdots, k$, as shown in Figure 1. We discretize each edge using a fitted mesh approach with $N_i + 1$ number of mesh points to discretize the domain $\bar{\Omega}_i = \bar{\Omega}_i^- \cup \bar{\Omega}_i^+$.

Now, partition the domain $\bar{\Omega}_i^- = [0, d_i]$ into following three sub-intervals

$$[0, \tau_{i,1}], \;\; [\tau_{i,1}, d_i - \tau_{i,1}] \;\; \text{and} \;\; [d_i - \tau_{i,1}, d_i],$$

and the domain $\bar{\Omega}_i^+ = [d_i, 1]$ into following three sub-intervals

$$[d_i, d_i + \tau_{i,2}], \quad [d_i + \tau_{i,2}, 1 - \tau_{i,2}] \quad \text{and} \quad [1 - \tau_{i,2}, 1],$$

where

$$\tau_{i,1} = \min\left\{\frac{d_i}{4}, 2\sqrt{\frac{\varepsilon_i}{\delta_i}}\ln N_i\right\}, \quad \text{and} \quad \tau_{i,2} = \min\left\{\frac{1-d_i}{4}, 2\sqrt{\frac{\varepsilon_i}{\delta_i}}\ln N_i\right\}.$$

On the sub-intervals $[\tau_{i,1}, d_i - \tau_{i,1}]$ and $[d_i + \tau_{i,2}, 1 - \tau_{i,2}]$, a uniform mesh with $N_i/4$ mesh-intervals are placed, whereas on the sub-intervals $[0, \tau_{i,1}], [d_i - \tau_{i,1}, d_i]$, $[d_i, d_i + \tau_{i,2}]$ and $[1 - \tau_{i,2}, 1]$, a uniform mesh with $N_i/8$ mesh-intervals are placed. So, we define the discrete domain as follows:

$$\Omega_i^{N_i} = \{x_{i,j} : 1 \le j \le N_i/2 - 1\} \cup \{x_{i,j} : N_i/2 + 1 \le j \le N_i - 1\}.$$

Now consider $\Omega_i^{N_i} = \Omega_{i,1}^{N_i} \cup \Omega_{i,2}^{N_i}$, where $\Omega_{i,1}^{N_i} = \left\{x_{i,j}\right\}_{j=1}^{\frac{N_i}{2}-1}$, $\Omega_{i,2}^{N_i} = \left\{x_{i,j}\right\}_{j=\frac{N_i}{2}+1}^{N_i-1}$, $x_{i,0} = 0$, $x_{i,N_i} = 1$ and $\Omega_{i*}^{N_i} = \Omega_i^{N_i} \cup \{x_{i,N_i}\}$. It is clear that $x_{i,\frac{N_i}{2}} = d_i$. Therefore, we consider the whole discretize domain for ith edge denoted by $\bar{\mathbb{D}}_{h_i}^{N_i} = \left\{x_{i,j}\right\}_{j=0}^{N_i}$, the step size is defined by $h_{i,j} = x_{i,j+1} - x_{i,j}$.

4.1. Discrete problem

Consider that $U_{i,j} = U_i(x_{i,j})$ be the numerical solution on the ith edge of the k-star graph domain on the fitted mesh. The following expressions offer the discrete formulation corresponding to Eqs (2.1)–(2.4):

$$T_{\varepsilon_i}^{N_i} U_{i,j} := -\varepsilon_i \delta^2 U_{i,j} + f_i\left(x_{i,j}, U_{i,j}\right) = g_i(x_{i,j}), \ x_{i,j} \in \Omega_i^{N_i}, \ \text{for all } i, \tag{4.1}$$

$$T_{d_i}^{N_i} U_{i,N_i/2} := D_*^+ U_{i,N_i/2} - D_*^- U_{i,N_i/2} = 0, \ \text{for all } \ i, \tag{4.2}$$

$$T_{0_i}^{N_i} U_{i,0} := -\mu_{i,1} U_{i,0} + \mu_{i,2} D_*^+ U_{i,0} = \psi_i, \ \text{for all } \ i, \tag{4.3}$$

$$T_{N_i}^{N_i} U_i(x_{i,N_i}) = T_{N_m}^{N_m} U_m(x_{i,N_m}) := u^J, \ \text{ for } \ i \ne m, \ \text{for all } i, m, \tag{4.4}$$

$$\sum_{i=1}^{k} \varepsilon_i D_*^- U_i(x_{i,N_i}) = 0, \tag{4.5}$$

where $i, m = 1, 2, \cdots, k$, $\delta^2 U_{i,j} = \dfrac{2}{h_{i,j+1} + h_{i,j}}\left(\frac{U_{i,j+1} - U_{i,j}}{x_{i,j+1} - x_{i,j}} - \frac{U_{i,j} - U_{i,j-1}}{x_{i,j} - x_{i,j-1}}\right)$, $D_*^+ U_{i,j} = \frac{-U_{i,j+2} + 4U_{i,j+1} - 3U_{i,j}}{2h_{i,j+1}}$ (three-point approximation at right hand side) and $D_*^- U_{i,j} = \frac{U_{i,j-2} - 4U_{i,j-1} + 3U_{i,j}}{2h_{i,j}}$ (three point approximation at left hand side). Note that; the order of convergence for Kirchhoff's condition at the junction point; is also almost second-order by using the derivative bound from Remark 1, i.e.,

$$\sum_{i=1}^{k} \varepsilon_i \left| u'(1) - \frac{U_{i,N_i-2} - 4U_{i,N_i-1} + 3U_{i,N_i}}{2h_{i,N_i}} \right| \le C\left(\sum_{i=1}^{k} h_{i,N_i}^2\right) = C\left(\sum_{i=1}^{k} N_i^{-2} \ln^2 N_i\right), \ \text{C is a constant.} \tag{4.6}$$

Consider that $\mathcal{T}_{\varepsilon_i}^{N_i}$ is the Fréchet derivative [43] of $T_{\varepsilon_i}^{N_i}$. Hence, it satisfies the following linear problem:

$$\mathcal{T}_{\varepsilon_i}^{N_i} U_{i,j} := -\varepsilon_i \delta^2 U_{i,j} + a_{i,j} U_{i,j} = g_{i,j}, \ \text{ on } \Omega_i^{N_i}, \ \text{ for } \ i = 1, 2, \cdots, k, \tag{4.7}$$

$$T_{d_i}^{N_i} U_{i,N_i/2} := D_*^+ U_{i,N_i/2} - D_*^- U_{i,N_i/2} = 0, \ \text{ for } \ i = 1, 2, \cdots, k, \tag{4.8}$$

$$T_{0_i}^{N_i} U_{i,0} := -\mu_{i,1} U_{i,0} + \mu_{i,2} D_*^+ U_{i,0} = \psi_i, \quad \text{for } i = 1, 2, \cdots, k, \tag{4.9}$$

$$T_{N_i}^{N_i} U_{i,N_i} = T_{N_m}^{N_m} U_{m,N_m} := u^J, \quad \text{for } i \neq m, \text{ and } i, m = 1, 2, \cdots, k, \tag{4.10}$$

$$\sum_{i=1}^{k} \varepsilon_i D_*^- U_{i,N_i} = 0, \tag{4.11}$$

where $a_i(x_{i,j}) = \frac{\partial f_i}{\partial u_i}\left(x_{i,j}, \xi_j\right)$ is provided through the mean value theorem and $\mathcal{T}_{\varepsilon_i}^{N_i}$ is a linear operator. Note that we use the three-point discretization at the left and right boundary points and the point of discontinuity (i.e., $x_{i,N_i/2} = d_i$).

At the point $x_{i,N_i/2} = d_i$, we use the difference operator $T_{d_i}^{N_i}$ from [44], i.e.,

$$T_{d_i}^{N_i} U_{i,N_i/2} := \frac{-U_{i,N_i/2+2} + 4U_{i,N_i/2+1} - 3U_{i,N_i/2}}{2h_{i,N_i/2+1}} - \frac{U_{i,N_i/2-2} - 4U_{i,N_i/2-1} + 3U_{i,N_i/2}}{2h_{i,N_i/2}} = 0, \tag{4.12}$$

where $h_{i,N_i/2+1}$, and $h_{i,N_i/2}$ are the right and left step sizes of the point $x_{N_i/2}$ and $h_{i,N_i/2+1} = 8\tau_{i,2}/N_i$ and $h_{i,N_i/2} = 8\tau_{i,1}/N_i$.

Similarly, for the left boundary point, we employ the right-hand side three-point approximation

$$T_{0_i}^{N_i} U_{i,0} := -\mu_{i,1} U_{i,0} + \mu_{i,2} \left[\frac{-U_{i,2} + 4U_{i,1} - 3U_{i,0}}{2h_{i,1}} \right] = \psi_i, \tag{4.13}$$

and at the right boundary point, we discretize Kirchhoff's condition using the following three-point approximation

$$\sum_{i=1}^{k} \varepsilon_i \left[\frac{U_{i,N_i-2} - 4U_{i,N_i-1} + 3U_{i,N_i}}{2h_{i,N_i}} \right] = 0. \tag{4.14}$$

Therefore, we get the following:

$$\mathcal{T}_{H,\varepsilon_i}^{N_i} U_{i,j} = \begin{cases} \mathcal{T}_{\varepsilon_i}^{N_i} U_{i,j}, & \text{for } j \neq \frac{N_i}{2}, \\ T_{d_i}^{N_i} U_{i,j}, & \text{for } j = \frac{N_i}{2}. \end{cases} \tag{4.15}$$

By Eqs (4.13) and (4.14) and the continuity condition (4.10), the matrix corresponding to Eqs (4.12)–(4.14) is not an M-matrix. To assure the invertibility of the discrete system through the M-matrix criterion, we must transform Eqs (4.12)–(4.14) using Eq (4.7) as follows:

$$U_{i,N_i/2+2} = \Bigg(- g_{i,N_i/2+1} + a_{i,N_i/2+1} U_{i,N_i/2+1} + \frac{\varepsilon_i}{h_{i,N_i/2+1}} \frac{U_{i,N_i/2+1} - U_{i,N_i/2}}{h_{i,N_i/2+1}} + \frac{\varepsilon_i}{h_{i,N_i/2+1}^2} U_{i,N_i/2+1} \Bigg) \frac{h_{i,N_i/2+1}^2}{\varepsilon_i}, \tag{4.16}$$

$$U_{i,N_i/2-2} = \Bigg(- g_{i,N_i/2-1} + a_{i,N_i/2-1} U_{i,N_i/2-1} - \frac{\varepsilon_i}{h_{i,N_i/2}} \frac{U_{i,N_i/2} - U_{i,N_i/2-1}}{h_{i,N_i/2}} + \frac{\varepsilon_i}{h_{i,N_i/2}^2} U_{i,N_i/2-1} \Bigg) \frac{h_{i,N_i/2}^2}{\varepsilon_i}, \tag{4.17}$$

$$U_{i,2} = \left(-g_{i,1}h_{i,1} + \left(\frac{2\varepsilon_i + a_{i,1}h_{i,1}^2}{h_{i,1}}\right)U_{i,1} - \frac{\varepsilon_i}{h_{i,1}}U_{i,0}\right)\frac{h_{i,1}}{\varepsilon_i}, \tag{4.18}$$

$$U_{i,N_i-2} = \frac{h_{i,N_i}}{\varepsilon_i}\left(-g_{i,N_i-1}h_{i,N_i} - \frac{\varepsilon_i}{h_{i,N_i}}U_{i,N_i} + \left(\frac{2\varepsilon_i + a_{i,N_i-1}h_{i,N_i}^2}{h_{i,N_i}}\right)U_{N_i-1}\right). \tag{4.19}$$

For simplicity, we consider that $h_{i,N_i/2+1} = h_{i,N_i/2} = h_i$. After using the values $U_{i,N_i/2+2}$ and $U_{i,N_i/2-2}$ in Eq (4.12), we obtain

$$\begin{aligned} T_{D_i}^{N_i}U_{i,N_i/2} :&= \frac{1}{2h_i}\left[-\left(2 - \frac{a_{i,N_i/2-1}h_i^2}{\varepsilon_i}\right)U_{i,N_i/2-1} + 4U_{i,N_i/2} - \left(2 - \frac{a_{i,N_i/2+1}h_i^2}{\varepsilon_i}\right)U_{i,N_i/2+1}\right] \\ &= \frac{h_i}{2\varepsilon_i}\left(g_{i,N_i/2+1} + g_{i,N_i/2-1}\right). \end{aligned} \tag{4.20}$$

Consider that $h_{i,N_i} = h_{i,1} = H_i$ and from Eqs (4.18) and (4.13), we get

$$\begin{aligned} T_{\pi_i}^{N_i}U_{i,0} :&= \frac{1}{2H_i}\left[-\left(2 - \frac{a_1H_i^2}{\varepsilon_i}\right)\mu_{i,2}U_{i,1} + \left(2\mu_{i,1}H_i + 2\mu_{i,2}\right)U_{i,0}\right] \\ &= \frac{\mu_{i,2}H_i}{2\varepsilon_i}g_{i,1} - \psi_i. \end{aligned} \tag{4.21}$$

and from Eq (4.19) and Kirchhoff's condition (4.14), we get

$$\sum_{i=1}^{k}\frac{\varepsilon_i}{2H_i}\left[-\left(2 - \frac{a_{i,N_i-1}H_i^2}{\varepsilon_i}\right)U_{i,N_i-1} + 2U_{i.N_i}\right] = \sum_{i=1}^{k}\frac{H_i}{2}g_{i,N_i-1}. \tag{4.22}$$

Now, we define the discrete operator as follows:

$$\mathcal{T}_{M,\varepsilon_i}^{N_i}U_{i,j} = \begin{cases} \mathcal{T}_{\varepsilon_i}^{N_i}U_{i,j}, & \text{for } j \neq \frac{N_i}{2}, \\ T_{D_i}^{N_i}U_{i,j}, & \text{for } j = \frac{N_i}{2}, \end{cases}$$

and

$$\tilde{g}_{i,j} = \begin{cases} g_{i,j}, & \text{for } j \neq \frac{N_i}{2}, \\ \frac{h_i}{2\varepsilon_i}\left(g_{i,j+1} + g_{i,j-1}\right), & \text{for } j = \frac{N_i}{2}. \end{cases}$$

Then, we have the following system of equations:

$$\mathcal{T}_{M,\varepsilon_i}^{N_i}U_{i,j} = \tilde{g}_{i,j}, \text{ for } i = 1, 2, \cdots, k, \text{ and } j = 1, \cdots, N_i - 1, \tag{4.23}$$

$$T_{\pi_i}^{N_i}U_{i,0} = \frac{\mu_{i,2}H_i}{2\varepsilon_i}g_{i,1} - \psi_i, \tag{4.24}$$

$$T_{N_i}^{N_i}U_{i,N_i} = T_{N_m}^{N_m}U_{m,N_m} := u^J \text{ (unknown)}, \text{ for } i \neq m, \text{ and } i, m = 1, 2, \cdots, k, \tag{4.25}$$

with the transformed Kirchoff condition

$$\sum_{i=1}^{k} \frac{\varepsilon_i}{2H_i}\left[-\left(2-\frac{a_{i,N_i-1}H_i^2}{\varepsilon_i}\right)U_{i,N_i-1}+2U_{i,N_i}\right]=\sum_{i=1}^{k}\frac{H_i}{2}g_{i,N_i-1}. \tag{4.26}$$

Lemma 2. *Assume that* $N_i^2/\ln^2 N_i \geq 128\frac{\delta_i^*}{\delta_i}$, *where* $\delta_i^* = \max_{x\in e_i} a_i(x)$ *and* $\delta_i = \min_{x\in e_i} a_i(x)$. *Then, the operator* $\mathcal{T}_{M,\varepsilon_i}^{N_i}$ *defined in Eq (4.23), with the boundary conditions (4.24)–(4.26), will lead to an M-matrix.*

Proof. By Eqs (4.20)–(4.22) and (2.5), it is clear that $\frac{a_{i,j}h_i^2}{\varepsilon_i} > 0$, for $j = N_i/2-1, N_i/2+1$ and $\frac{a_{i,j}H_i^2}{\varepsilon_i} > 0$ for $j = 1, N_i-1$. Hence, the discretization produces an M-matrix, provided $\left(2-\frac{a_{i,j}h_i^2}{\varepsilon_i}\right)\geq 0$, and $\left(2-\frac{a_{i,j}H_i^2}{\varepsilon_i}\right)\geq 0$. We use a central difference scheme except for the boundary and discontinuous points. Therefore, we get

$$\frac{N_i^2}{\ln^2 N_i} \geq 32\frac{\delta_i^*}{\delta_i} \quad \text{and} \quad \frac{N_i^2}{\ln^2 N_i} \geq 128\frac{\delta_i^*}{\delta_i}.$$

Thus, the operator $\mathcal{T}_{M,\varepsilon_i}^{N_i}$ satisfies the discrete maximum principle on each edge of the k-star graph. Therefore, by consequences of the discrete maximum principle, the discrete solution is stable in the k-star graph domain $\mathcal{G}$. Then, the graph Laplacian for the discrete graph produces an M-matrix and satisfies the discrete maximum principle [33, 45]. Thus, Eqs (4.23)–(4.26) lead to a unique solution as describes an invertible M-matrix.

Remark 2. *Here, we are specifying the conditions for individual edges of the k-star graph (Figure 1). The boundary conditions for the outer vertices will remain unchanged. However, the continuity and Kirchhoff's conditions at the junction point will not apply to single edges. For instance, we consider a Dirichlet-type boundary condition at the junction point, where* u^J *will be treated as a known value at the boundary (junction point).*

4.1.1. Discrete stability result

Lemma 3. *On each edge* e_i *with* $1 \leq i \leq k$, *let us denote* $\Psi_{i,j}$ *as a mesh function such that* $\Psi_{i,0} = 0$, *and* $\Psi_{i,N_i} = u^J$. *Then,*

$$|\Psi_{i,j}| \leq \frac{1}{\delta_i}\max_{1\leq j\leq N_i-1}\left|\mathcal{T}_{M,\varepsilon_i}^{N_i}\Psi_{i,j}\right| + \left|u^J\right|, \quad \textit{for} \quad 0 \leq j \leq N_i.$$

Proof. Let $\Phi_{i,j}^{\pm}$ be mesh functions defined as $\Phi_{i,j}^{\pm} = \frac{x_{i,j}}{\delta_i d_i}\max_{1\leq j\leq N_i-1}|\mathcal{T}_{M,\varepsilon_i}^{N_i}\Psi_{i,j}| + |u^J| \pm \Psi_{i,j}$, $0 \leq j \leq N_i/2$ and $\Phi_{i,j}^{\pm} = \frac{(1-x_{i,j})}{\delta_i(1-d_i)}\max_{1\leq j\leq N_i-1}|\mathcal{T}_{M,\varepsilon_i}^{N_i}\Psi_{i,j}| + |u^J| \pm \Psi_{i,j}$, $N_i/2 < j \leq N_i$. It is clear that $\Phi_{i,0}^{\pm} > 0$ and $\Phi_{i,N_i}^{\pm} > 0$. Again, $\mathcal{T}_{M,\varepsilon_i}^{N_i}\Phi_{i,j}^{\pm} \geq 0$, for $1 \leq j \leq N_i - 1$.

Hence, by using the discrete maximum principle [33], we get

$$|\Psi_{i,j}| \leq \frac{1}{\delta_i}\max_{1\leq j\leq N_i-1}\left|\mathcal{T}_{M,\varepsilon_i}^{N_i}\Psi_{i,j}\right| + \left|u^J\right|, \quad \text{for} \quad 0 \leq j \leq N_i.$$

4.2. Convergence analysis

In this section, we provide the convergence result for each edge of the k-star graph domain.

Theorem 5. *On each edge e_i of the k-star graph domain, let $u_{i,0}$ be the solution of the problem (2.1) at the left boundary point, and $U_{i,0}$ be the solution of the corresponding discrete problem (4.7) at the left boundary point. Then,*

$$\sup_{0<\epsilon_i\leq 1} \|U_{i,0} - u_{i,0}\| \leq CN_i^{-2} \ln^2 N_i,$$

where C is independent of ε_i and N_i.

Proof. At the left boundary point $x_{i,0} = 0$, we have

$$\begin{aligned}
\left|T_{\pi_i}^{N_i}(U_{i,0} - u_{i,0})\right| &= \left|\left(\frac{\mu_{i,2}h_i}{2\varepsilon_i}g_{i,1} - \psi_i\right) - T_{\pi_i}^{N_i}u_{i,0}\right| \\
&\leq \left|T_{0_i}^{N_i}u_{i,0} - \mu_{i,2}u'_{i,0}\right| + C\left|T_{0_i}^{N_i}u_{i,1} - g_{i,1}\right| \\
&\leq \mu_{i,2}\left|\frac{-u_{i,2} + 4u_{i,1} - 3u_{i,0}}{2h_i} - u'_{i,0}\right| + C\left|T_{0_i}^{N_i}u_{i,1} - T_{\varepsilon_i}u_{i,1}\right| \\
&\leq C\mu_{i,2}h_{i,1}^2\left|u_i'''(0)\right| \\
&= CN_i^{-2}\ln^2 N_i.
\end{aligned}$$

Hence, we get the following by using Lemma 3

$$\left|U_{i,0} - u_{i,0}\right| \leq CN_i^{-2}\ln^2 N_i.$$

The case $\mu_{i,2} = \varepsilon_i$ leads to the same result based on a suitable choice of a suitable barrier function. Note that the derivatives are bound by $C\varepsilon_i^{-3/2}$ for this case (see Remark 1). However, the convergence proof will be simpler as $\mu_{i,2} = \varepsilon_i$.

Theorem 6. *On each edge e_i of the k-star graph domain, let u_i be the solution of the problem (2.1) , and U_i be the solution of the corresponding discrete problem (4.7). Then,*

$$\sup_{0<\epsilon_i\leq 1} \|U_i - u_i\|_{\Omega_{i*}^{N_i}} \leq CN_i^{-2}\ln^2 N_i, \quad on \quad \Omega_{i*}^{N_i},$$

where C is independent of ε_i and N_i.

Proof. We consider the following two cases to prove this theorem.

Case I: Consider $\mu_{i,2}$ as a constant. Here, we decompose the discrete solution into a regular component $R_i(x_{i,j})$ and a singular component $S_i(x_{i,j})$, such that

$$U_i(x_{i,j}) = R_i(x_{i,j}) + S_i(x_{i,j}),$$

where $R_i(x_{i,j})$ is the solution of the non-homogeneous problem and $S_i(x_{i,j})$ is the solution of the homogeneous problem [46]. Correspondingly, the error $(U_i - u_i)(x_{i,j})$ can be decomposed as

$$(U_i - u_i)(x_{i,j}) = (R_i - r_i)(x_{i,j}) + (S_i - s_i)(x_{i,j}).$$

From the original problem and the discretized problem, we get

$$\begin{aligned}\left|\mathcal{T}_{\varepsilon_i}^{N_i}(U_i-u_i)\left(x_{i,j}\right)\right| &= \left|\mathcal{T}_{\varepsilon_i}^{N_i}\left((R_i-r_i)+(S_i-s_i)\right)(x_{i,j})\right| \\ &\le \left|\left(T_{\varepsilon_i}^{N_i}-T_{\varepsilon_i}\right)r_i\left(x_{i,j}\right)\right| + \left|\left(T_{\varepsilon_i}^{N_i}-T_{\varepsilon_i}\right)s_i\left(x_{i,j}\right)\right| \\ &\le \varepsilon_i\left(\left|\left(\delta^2-\frac{d^2}{dx^2}\right)r_i\left(x_{i,j}\right)\right| + \left|\left(\delta^2-\frac{d^2}{dx^2}\right)s_i\left(x_{i,j}\right)\right|\right).\end{aligned}$$

Now, we find the error estimate separately. Let us first derive it for the regular component. Note

$$\begin{aligned}\varepsilon_i\left|\left(\delta^2-\frac{d^2}{dx^2}\right)r_i\left(x_{i,j}\right)\right| &\le \begin{cases} C_i\varepsilon_i\left(h_{i,j+1}+h_{i,j}\right)\max_j\left|r_i^{(3)}\left(x_{i,j}\right)\right|, & x_{i,j}\in\{\tau_{i,1},d_i-\tau_{i,1},d_i+\tau_{i,2},1-\tau_{i,2}\},\\ C_i\varepsilon_i\left(h_{i,j+1}+h_{i,j}\right)^2\max_j\left|r_i^{(4)}\left(x_{i,j}\right)\right|, & \text{otherwise,}\end{cases}\\ &\le \begin{cases} C_i\varepsilon_i N_i^{-1}, & x_{i,j}\in\{\tau_{i,1},d_i-\tau_{i,1},d_i+\tau_{i,2},1-\tau_{i,2}\},\\ C_i\sqrt{\varepsilon_i}N_i^{-2}, & \text{otherwise.}\end{cases}\end{aligned}$$

Here, we use the piecewise uniform mesh and its property $h_{i,j+1}+h_{i,j}\le 2N^{-1}$, and have applied Theorem 4. Now, let us introduce the function

$$\Theta_{i,j}=C_iN_i^{-2}+C_iN_i^{-2}\tau_{i,1}\begin{cases}\frac{x_{i,j}}{\tau_{i,1}}, & 0<x_{i,j}\le\tau_{i,1},\\ 1, & \tau_{i,1}\le x_{i,j}\le d_i-\tau_{i,1},\\ \frac{d_i-x_{i,j}}{\tau_{i,1}}, & d_i-\tau_{i,1}\le x_{i,j}<d_i,\end{cases}$$ on the interval $(0,d_i)$ and introduce the function $\Theta_{i,j}=C_iN_i^{-2}+C_iN_i^{-2}\tau_{i,2}\begin{cases}\frac{x_{i,j}-d_i}{\tau_{i,2}}, & d_i<x_{i,j}\le d_i+\tau_{i,2},\\ 1, & d_i+\tau_{i,2}\le x_{i,j}\le 1-\tau_{i,2},\\ \frac{1-x_{i,j}}{\tau_{i,2}}, & 1-\tau_{i,2}\le x_{i,j}\le 1,\end{cases}$ on the interval $(d_i,1]$. Note that $\Theta_{i,j}\le C_i\sqrt{\varepsilon_i}N_i^{-2}\ln N_i$ and

$$\mathcal{T}_{\varepsilon_i}^{N_i}\Theta_{i,j}\ge\begin{cases}C_i(\varepsilon_iN_i^{-1}+N_i^{-2}), & x_{i,j}\in\{\tau_{i,1},d_i-\tau_{i,1},d_i+\tau_{i,2},1-\tau_{i,2}\},\\ C_i\sqrt{\varepsilon_i}N_i^{-2}, & \text{otherwise.}\end{cases}$$

Now, consider the barrier function

$$\Phi_{i,j}=\Theta_{i,j}\pm\varepsilon_i\left[\left(\delta^2-\frac{d^2}{dx^2}\right)r_i\left(x_{i,j}\right)\right].$$

By the discrete maximum principle [45], we obtain

$$\varepsilon_i\left|\left(\delta^2-\frac{d^2}{dx^2}\right)r_i\left(x_{i,j}\right)\right|\le C_i\sqrt{\varepsilon_i}N_i^{-2}\ln N_i. \tag{4.27}$$

Now, we decompose the singular component S_i along the interval $(0,d)$ and $(d,1]$; as follows

$$S_i=S_{L_i}+S_{R_i},$$

where S_{L_i} is defined on $(0,d)$; and S_{R_i} is defined on $(d,1]$; and are given by

$$\mathcal{T}_{\varepsilon_i}^{N_i}S_{L_i}(x_{i,j})=0,\quad T_{0_i}S_{L_i}(0)=T_{0_i}s_{L_i}(0),\quad T_{1_i}S_{L_i}(d-)=T_{1_i}s_{L_i}(d-),$$

$$\mathcal{T}^{N_i}_{\varepsilon_i} S_{R_i}(x_{i,j}) = 0, \quad T_{0_i} S_{R_i}(d+) = T_{0_i} s_{R_i}(d+), \quad T_{1_i} S_{R_i}(1) = T_{1_i} s_{R_i}(1).$$

Note that either $\tau_{i,1} = \frac{d_i}{4}$, and $\tau_{i,2} = \frac{1-d_i}{4}$, or $\tau_{i,1} = \tau_{i,2} = 2\sqrt{\frac{\varepsilon_i}{\delta_i}} \ln N_i \leq \frac{d_i}{4}$. Thur, if $x_{i,j} = d_i = \frac{1}{2}$, we have $\tau_{i,1} = \tau_{i,2}$. For $\tau_{i,1} = \tau_{i,2} = \frac{1}{8}$, the mesh will be uniform throughout the domain $\Omega^{N_i}_{i*}$.

Hence, by using the argument in [47] for the singular component S_{L_i} on $\Omega^{N_i}_{i,1}$, we get

$$\varepsilon_i \left| \left(\delta^2 - \frac{d^2}{dx^2} \right) S_{L_i}\left(x_{i,j}\right) \right| \quad \leq \quad C N_i^{-2} \ln^2 N_i. \tag{4.28}$$

Similarly, for the singular component S_{R_i} on $\Omega^{N_i}_{i,2} \cup \{x_{i,N_i}\}$, we get

$$\varepsilon_i \left| \left(\delta^2 - \frac{d^2}{dx^2} \right) S_{R_i}\left(x_{i,j}\right) \right| \quad \leq \quad C N_i^{-2} \ln^2 N_i. \tag{4.29}$$

Combining Eqs (4.28) and (4.29), we get

$$\left| \mathcal{T}^{N_i}_{\varepsilon_i} \left(S_i - s_i \right)(x_{i,j}) \right| \leq C N_i^{-2} \ln^2 N_i. \tag{4.30}$$

Hence, by utilizing Lemma 3, from Eqs (4.27) and (4.30), we obtain

$$|U_i - u_i| \leq C N_i^{-2} \ln^2 N_i.$$

Case II: Here, we assume $\mu_{i,2} = \varepsilon_i$, we determine the error estimate in a similar way as given in [33].

Theorem 7. *On each edge e_i of the k-star graph, let $u_{i,N_i/2}$ be the solution of the problem (2.1) at the discontinuity point, and $U_{i,N_i/2}$ be the solution of the corresponding discrete problem (4.7) at the discontinuity point. Then,*

$$\sup_{0<\epsilon_i\leq 1} \|U_{i,N_i/2} - u_{i,N_i/2}\| \leq C N_i^{-2} \ln^2 N_i,$$

where C is independent of ε_i and N_i.

Proof. Let us take the case that $\mu_{i,2}$'s are positive constants. Then, we have the following consistency estimate at the point of discontinuity $x_{i,N_i/2} = d_i$:

$$\begin{aligned}
\left| \mathcal{T}^{N_i}_{M,\varepsilon_i} u_{i,N_i/2} - \frac{h_i}{2\varepsilon_i} g_{i,N_i/2+1} - \frac{h_i}{2\varepsilon_i} g_{i,N_i/2-1} \right| &= \left| T^{N_i}_{D_i} u_{i,N_i/2} - \frac{h_+}{2\varepsilon_i} g_{i,N_i/2+1} - \frac{h_-}{2\varepsilon_i} g_{i,N_i/2-1} \right| \\
&\leq \left| T^{N_i}_{d_i} u_{i,N_i/2} + [u'](d_i) \right| \\
&+ \frac{h_+}{2\varepsilon_i} \left| \mathcal{T}^{N_i}_{\varepsilon_i} u_{i,N_i/2+1} - g_{i,N_i/2+1} \right| \\
&+ \frac{h_i}{2\varepsilon_i} \left| \mathcal{T}^{N_i}_{\varepsilon_i} u_{i,N_i/2-1} - g_{i,N_i/2-1} \right| \\
&\leq \left| \frac{-u_{i,N_i/2+2} + 4u_{i,N_i/2+1} - 3u_{i,N_i/2}}{2h_i} - u'_{i,N_i/2} \right| \\
&+ \left| \frac{u_{i,N_i/2-2} - 4u_{i,N_i/2-1} + 3u_{i,N_i/2}}{2h_i} - u'_{i,N_i/2} \right| \\
&+ C_i \left| T_{\varepsilon_i} u_{i,N_i/2-1} - \mathcal{T}^{N_i}_{\varepsilon_i} U_{i,N_i/2-1} \right| \\
&+ C_i \left| T_{\varepsilon_i} u_{i,N_i/2+1} - \mathcal{T}^{N_i}_{\varepsilon_i} U_{i,N_i/2+1} \right| \\
&\leq C_i h^2_{i,j} \left| u'''_i(\xi_{i,j}) \right|.
\end{aligned}$$

Hence, by applying Theorem 4 with $h_i = 8\sqrt{\frac{\varepsilon_i}{\delta_i}}N_i^{-1}\ln N_i$, we get

$$\left|U_{i,N_i/2} - u_{i,N_i/2}\right| \le CN_i^{-2}\ln^2 N_i. \tag{4.31}$$

For case $\mu_{i,2} = \varepsilon_i$, let us consider the barrier function η_{d_i}, defined by

$$-\varepsilon_i\delta^2\eta_{d_i}(x_{i,j}) + \delta_i\eta_{d_i}(x_{i,j}) = 0, \text{ for all } x_{i,j} \in \Omega_i^{N_i},$$

$$\eta_{d_i}(0) = 0, \quad \eta_{d_i}(d_i) = 1, \quad \eta_{d_i}(1) = 0.$$

From the discrete maximum principle on each intervals $[0, d_i]$ and $[d_i, 1]$, one can easily get

$$0 \le \eta_{d_i} \le 1,$$

and

$$\mathcal{T}_{\varepsilon_i}^{N_i}\eta_{d_i}(x_{i,j}) = (a(x_{i,j}) - \delta_i)\eta_{d_i}(x_{i,j}) \ge 0, \text{ for all } x_{i,j} \in \Omega_i^{N_i} \cup \{d_i\}.$$

Define the ancillary continuous functions $w_{i,1}$, $w_{i,2}$ by

$$-\varepsilon_i w_{i,1}'' + \delta_i w_{i,1} = 0, \quad w_{i,1}(0) = 0, \quad w_{i,1}(d_i) = 1,$$

$$-\varepsilon_i w_{i,2}'' + \delta_i w_{i,2} = 0, \quad w_{i,2}(d_i) = 1, \quad w_{i,2}(1) = 0.$$

In addition, define

$$\tilde{w}(x_{i,j}) = \begin{cases} w_{i,1}(x_{i,j}), & \text{for } x_{i,j} \in (0, d_i), \\ w_2(x_{i,j}), & \text{for } x_{i,j} \in (d_i, 1). \end{cases}$$

Hence, from [45], we get the following estimate

$$T_{d_i}^{N_i}\tilde{w} \le \frac{-C}{\sqrt{\varepsilon_i}}.$$

Therefore, for the intervals $[0, d_i]$ and $[d_i, 1]$ respectively, we have the following estimates

$$|\eta_{d_i}(x_{i,j}) - w_{i,1}(x_{i,j})| \le CN_i^{-2}\ln^2 N_i, \quad j \le N/2,$$

$$|\eta_{d_i}(x_{i,j}) - w_{i,2}(x_{i,j})| \le CN_i^{-2}\ln^2 N_i, \quad j \ge N_i/2.$$

For $j = N_i/2$,

$$\begin{aligned} T_{d_i}^{N_i}\eta_{d_i}(d_i) &= \frac{-\eta_{d_i}(d_i + 2h_{i,N_i/2+1}) + 4\eta_{d_i}(d_i + h_{i,N_i/2+1}) - 3\eta_{d_i}(d_i)}{2h_{i,N_i/2+1}} \\ &- \frac{\eta_{d_i}(d_i - 2h_{i,N_i/2-1}) - 4\eta_{d_i}(d_i - h_{i,N_i/2-1}) + 3\eta_{d_i}(d_i)}{2h_{i,N_i/2-1}} \\ &= T_{d_i}^{N_i}\tilde{w} \pm \frac{C_i h_{i,j}^2}{\varepsilon_i^{\frac{3}{2}}} \le \frac{-C_i}{\sqrt{\varepsilon_i}}. \end{aligned} \tag{4.32}$$

For sufficiently large N_i, let us consider the function

$$\mathbf{\Delta_i}(x_{i,j}) = C(N_i^{-1}\ln N_i)^2 + C\frac{h^2}{\varepsilon_i}\eta_{d_i}(x_{i,j}) \pm e_i(x_{i,j}).$$

Note that, for $i = N_i/2$

$$T_{d_i}^{N_i}\mathbf{\Delta_i}(d_i) \leq 0.$$

Hence, for sufficiently large N_i, we have

$$\left|U_{i,N_i/2} - u_{i,N_i/2}\right| \leq CN_i^{-2}\ln^2 N_i. \tag{4.33}$$

Hence, we get the required result from Eqs (4.31) and (4.33).

Theorem 8. *On each edge e_i of the k-star graph domain, let u_i be the solution of the problems (2.1) and (2.2), with the Dirichlet boundary condition (2.3) where u^J is known at the junction point, and U_i be the solution of the corresponding discrete problems (4.7)–(4.9) with the Dirichlet boundary condition (4.10) where u^J is known at the junction point. Then*

$$\sup_{0<\epsilon_i\leq 1} \|U_i - u_i\|_{\bar{\mathbb{D}}_{h_i}^{N_i}} \leq CN_i^{-2}\ln^2 N_i, \text{ on } \bar{\mathbb{D}}_{h_i}^{N_i},$$

where C is independent of ε_i and N_i.

Proof. Utilizing the Theorems 5–7, the desired result follows.

Remark 3. *The present numerical scheme provides an almost second-order parameter uniform convergence on piecewise uniform meshes; as depicted in Theorems 5–8. This order of accuracy is sharper than the numerical approximations, where we use upwind discretizations for mixed-type boundary conditions and the Kirchhoff law at the junction point. In addition, the logarithmic term inside the order of accuracy $O(N_i^{-2}\ln^2 N_i)$ cannot be removed if the continuous domain is replaced by a piecewise uniform mesh [48]. The simple structure of this mesh assumes the boundary and interior locations and their widths in advance. If this information is unavailable, one can use other kinds of adaptive moving meshes or equidistributed meshes, like in [17, 20, 21] to enhance the rate of accuracy. However, the adaptive mesh generation algorithms are complicated and these algorithms also increase the computational costs [22] for coupled systems, which can be greatly reduced by splitting of the coupled matrices [23], appearing in the original model.*

Now, we present the main result of this paper on the k-star graph, which gives the almost second-order ε_i-uniform estimate.

Theorem 9. *On the k-star graph domain, let u_ε be the solution of the problems (2.1)–(2.4), and U_ε be the solution of the corresponding discrete problems (4.7)–(4.11). Then,*

$$\sup_{0<\epsilon\leq 1} \|U_\varepsilon - u_\varepsilon\|_{\bar{\mathbb{D}}_h^{N_i}} \leq CN^{-2}\ln^2 N,$$

where $N_i = N$, over all edges; and C is independent of ε and N.

Proof. We have proved in Theorem 8 that an almost second-order error estimate holds throughout every edge of the k-star graph when u^J is known. In the present k-star graph domain, all the edges are connected at a single point on the boundary, known as the junction point, where the u^J is unknown. Thus, we need to solve the solution components over all edges simultaneously, instead of edge-wise, as u^J is unknown. Note that the continuity condition (2.3) for the continuous problem; is equivalent to

the continuity condition (4.10) at the discrete problem. In addition, to match the number of equations with the number of discrete variables, we need another equation, which will be given by the Kirchhoff equation (4.11). Hence, the number of variables of discrete problems matches the number of equations for the discrete problem along the k star graph domain. We have proved that the rate of accuracy along every edge is preserved up to $N_i^{-2}\ln^2 N_i$ in Theorem 8. This rate is also preserved for the present discretization of the Kirchhoff equation, see Eq (4.6). In addition, the discrete problems (4.23)–(4.26) is uniformly stable, as provided in Lemma 3. Hence, we can write the following:

Now, let U_ε and u_ε be the discrete and analytical solutions on the k-star graph, respectively. Then, the error estimate on the k-star graph is given by:

$$\sup_{0<\epsilon\leq 1} \|U_\varepsilon - u_\varepsilon\|_{\bar{\mathbb{D}}_h^{N_i}} \leq CN^{-2}\ln^2 N,$$

where $N^{-2}\ln^2 N = \max(N_i^{-2}\ln^2 N_i)$ for all $i = 1, 2, \ldots, k$, and C is a constant independent of ε and N, and $\bar{\mathbb{D}}_h^N$ represents the k-star graph domain.

Hence, the maximum global error on the entire k-star graph domain is independent of ε and bounded by $CN^{-2}\ln^2 N$.

5. Numerical experiments

In this section, we discuss the numerical experiments to verify the theoretical results, obtained in the earlier sections. Here, we consider the perturbation parameters from the set $\varepsilon = (\varepsilon_1, \varepsilon_2, \varepsilon_3)$ and use the same number of mesh intervals N for $k = 3$ star graph in Example 1. We take the singular perturbation parameters from the set $\mathbf{S} = \{2^{-(p-1)};\ p = 1, 2, \cdots, 40\}$, and discretize the problem having the transition parameters $\tau_1, \tau_2,$ and τ_3 on the 3-star graph. We compute the nodal errors of the approximate solution using the double mesh principle [17, 21] as follows:

$$E_i^N = \max_{\varepsilon_i\in\mathbf{S}} \max_{0\leq j\leq N} |U_{i,j}^{N,\varepsilon_i} - U_{i,j}^{2N,\varepsilon_i}|, \quad E^N = \max_{i=1,2,3}\{E_i^N\},$$

where $U_{i,j}^{N,\varepsilon_i}$ represents the approximate solution components at $x_{i,j}$ across the ith edge of the 3-star graph with $N + 1$ mesh points for each edge, and $U_{i,j}^{2N,\varepsilon_i}$ represents the solution with $2N + 1$ mesh points, obtained by bisecting the previous mesh points on each edge. The corresponding order of convergence is calculated as follows:

$$\rho_i^N = \log_2(E_i^N/E_i^{2N}), \quad \rho^N = \log_2(E^N/E^{2N}).$$

Example 1. *Let us consider the following nonlinear reaction-diffusion problem with discontinuous source terms on the* 3*-star graph over* $[0, 1]$ *(see Figure 2):*

$$T_{\varepsilon_1}u_1(x) := -\varepsilon_1 u_1'' + (1 - u_1^2)u_1 = \begin{cases} 0.1 - x(x - 0.5), & \text{for} \quad 0 \leq x < 0.5, \\ -0.2 - (x - 1)(x - 0.5), & \text{for} \quad 0.5 < x \leq 1, \end{cases} \tag{5.1}$$

$$T_{\varepsilon_2}u_2(x) := -\varepsilon_2 u_2'' + u_2 - 0.5 - (0.5 - u_2)^5 + e^{u_2^2} = \begin{cases} e^x, & \text{for } x < 0.5, \\ 1 - \log(|x - 0.5| + 1), & \text{for } x \geq 0.5, \end{cases} \tag{5.2}$$

$$T_{\varepsilon_3}u_3(x) := -\varepsilon_3 u_3'' + u_3 = \begin{cases} 0.7, & \text{for} \quad 0 \leq x < 0.5, \\ -0.6, & \text{for} \quad 0.5 < x \leq 1, \end{cases} \tag{5.3}$$

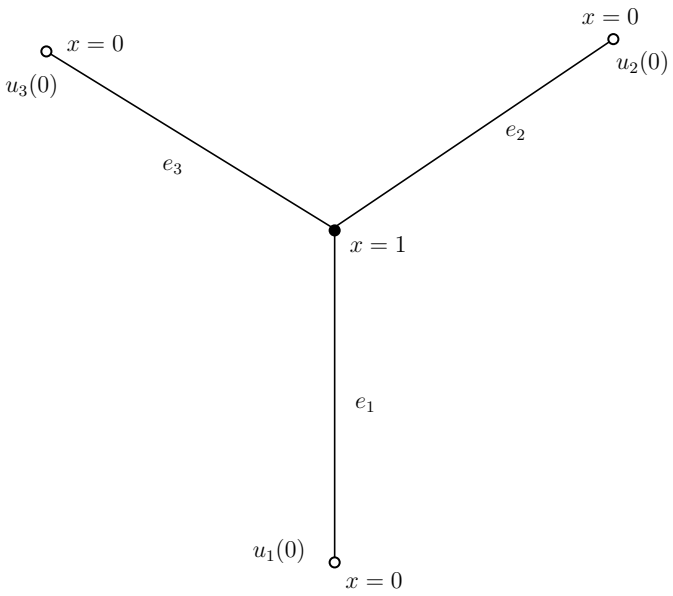

Figure 2. 3- Star Graph.

with any one of the boundary conditions at the free vertices

$$(\mathbf{a})\begin{cases} u_1(0) = 0, \\ u_2(0) = 0, \\ u_3(0) = 0, \end{cases} \quad (\mathbf{b})\begin{cases} 2u_1(0) - u_1'(0) = 1, \\ u_2(0) - 4u_2'(0) = 0, \\ 2u_3(0) - u_3'(0) = 1, \end{cases} \quad (\mathbf{c})\begin{cases} 2u_1(0) - \varepsilon_1 u_1'(0) = 1, \\ u_2(0) - 3\varepsilon_2 u_2'(0) = 3, \\ 2u_3(0) - \varepsilon_3 u_3'(0) = 8. \end{cases} \tag{5.4}$$

The continuity condition at the junction point is

$$u_1(1) = u_2(1) = u_3(1) = u^J, \tag{5.5}$$

where u^J is unknown (here, J stands for junction point), and Kirchhoff's condition at the junction point is

$$\sum_{i=1}^{3} \varepsilon_i u_i'(1) = 0. \tag{5.6}$$

We use Newton's quasi-linearization technique to linearize the given nonlinear problem. Let us first approximate Kirchhoff's junction law with the standard upwind scheme. At discontinuity points, we employ the scheme (4.8), and for Neumann conditions, a first-order upwind approximation of the derivative is utilized. Tables 1–3 depict the uniform errors of overall solution components and the corresponding linear accuracy of the numerical solution. Hence, it illustrates that the upwind scheme yields an almost first-order uniformly convergent approximate solution of the current Example 1.

Table 1. Uniform errors overall solution components across all edges of 3-star graph, and corresponding rate of convergences throughout the discrete domain, for Example 1(a).

N	64	128	256	512	1024
E^N	1.7498e-02	9.8782e-03	4.9769e-03	2.6413e-03	1.3748e-03
ρ^N	8.2487e-01	9.8900e-01	9.1400e-01	9.4203e-01	

Table 2. Uniform errors over all solution components across all edges of the 3-star graph, and corresponding rate of convergences throughout the discrete domain, for Example 1(b).

N	64	128	256	512	1024
E^N	6.0992e-03	3.1313e-03	1.4399e-03	6.6872e-04	3.2107e-04
ρ^N	9.6184e-01	1.1208	1.1065	1.0585	

Table 3. Uniform errors over all solution components across all edges of the 3-star graph, and corresponding rate of convergences throughout the discrete domain, for Example 1(c).

N	64	128	256	512	1024
E^N	2.2695e-02	1.5914e-02	9.8826e-03	5.7780e-03	3.2725e-03
ρ^N	5.1209e-01	6.8735e-01	7.7432e-01	8.2017e-01	

Moreover, we apply our proposed scheme, which utilizes a three-point scheme (4.9) for the first-order derivatives in Kirchhoff's junction law (4.11) and mixed boundary conditions. At the points of discontinuities, we employ a five-point scheme (4.8) for higher-order accuracy. We consider three different types of boundary conditions for Example 1: Dirichlet boundary conditions (5.4a), mixed boundary conditions (5.4b), and scaled mixed boundary conditions (5.4c). By applying this scheme, we obtain a higher-order accurate solution for each boundary condition. To justify this, we find the uniform maximum error on each edge of the 3-star graph domain. Then, we take the maximum of these errors over all edges of the 3-star graph domain to compute the uniform errors. Let us first discuss the Example 1 with the boundary conditions (5.4a): Table 4 shows that the maximum error estimate on the single edge e_1 for problem (5.1) with the boundary condition given in (5.4a), where $\varepsilon \in \mathbf{S}$. Similarly, Table 5 presents the maximum error for problem (5.2) on the edge e_2, with the boundary conditions (5.4a), where we take the perturbation parameters from the set $\varepsilon \in \mathbf{S}$. Analogously, Table 6 shows the maximum error for problem (5.3) on the edge e_3, with the boundary conditions (5.4a).

Table 4. Uniform maximum error and its rate of accuracy across the edge e_1 for component u_1 for Example 1(a) with $\varepsilon \in \mathbf{S}$.

N	64	128	256	512	1024
E_1^N	4.4593e-03	2.0357e-03	7.0952e-04	2.3028e-04	7.1749e-05
ρ_1^N	1.1633	1.5206	1.6234	1.6824	

Table 5. Uniform maximum error and its rate of accuracy across the edge e_2 for solution component u_2 for Example 1(a) with $\varepsilon \in \mathbf{S}$.

N	64	128	256	512	1024
E_2^N	4.0778e-03	1.4439e-03	4.9194e-04	1.5719e-04	4.8688e-05
ρ_2^N	1.4978	1.5534	1.6460	1.6909	

Table 6. Uniform maximum error and its rate of accuracy across the edge e_3 for solution component u_3 for Example 1(a) with $\varepsilon \in \mathbf{S}$.

N	64	128	256	512	1024
E_3^N	7.9016e-03	2.8153e-03	9.6233e-04	3.0754e-04	1.2652e-04
ρ_3^N	1.4889	1.5487	1.6458	1.2814	

Note that the nonlinear problems (5.1)–(5.3) are coupled at the junction point. Hence, we impose the continuity condition (5.5) and Kirchhoff's condition (5.6) to preserve the continuity of the solution, even though the source function is non-smooth. Now, we produce the effect of these conditions and their discretizations for the coupled system (1) with the boundary conditions (5.4a), continuity condition (5.5), and Kirchhoff's condition (5.6). This is shown in Table 7, where we also observe an almost second-order convergence overall perturbation parameters from the range $\varepsilon \in \mathbf{S}$.

Table 7. Uniform errors overall solution components across all edges of the 3-star graph, and corresponding rate of convergences throughout the discrete domain, for Example 1(a).

N	64	128	256	512	1024
E^N	7.9016e-03	2.8153e-03	9.6233e-04	3.0754e-04	1.2652e-04
ρ^N	1.4889	1.5487	1.6458	1.2814	

Next, we discuss the conditions at the free vertices of the 3-star graph. The maximum error and corresponding order of convergence on each edge of the 3-star graph are provided for this example, with the boundary conditions (5.4b), continuity condition (5.5), and Kirchhoff's condition (5.6). The results shown in Tables 8–10, clearly indicate almost second-order uniform convergence. The coupled system in this example with boundary conditions (5.4b) with (5.5) and (5.6), also demonstrates the almost second-order convergence, as presented in Table 11, for $\varepsilon \in \mathbf{S}$. Similarly, The results shown in Tables 12–14, clearly indicate almost second-order uniform convergence for each solution component u_1, u_2, and u_3 respectively for (5.4c) along with the (5.5) and (5.6). Finally, considering the mixed boundary conditions (5.4c), the numerical approximation for the coupled system of the 3-star graph (see Figure 1) shows the almost uniform second-order convergence, as seen in Table 15, for $\varepsilon \in \mathbf{S}$. Note that the obtained accuracy is higher than the discretizations, where the stiffness matrices are generated through the simple upwind two-point schemes for first-order derivatives. We want to note that the round-off errors can affect the order of accuracy when the tolerance is minimal, like 10^{-6}, and dominate the errors.

Table 8. Uniform maximum error and its rate of convergence across the whole domain for approximating solution component u_1 along edge e_1, for Example 1(b), with $\varepsilon \in \mathbf{S}$.

N	64	128	256	512	1024
E_1^N	1.1154e-02	7.1656e-03	2.3076e-03	7.9499e-04	2.9411e-04
ρ_1^N	0.63835	1.6347	1.5374	1.4346	

Table 9. Uniform maximum error and its rate of convergence across the edge e_2 for solution component u_2 for Example 1(b) with $\varepsilon \in \mathbf{S}$.

N	64	128	256	512	1024
E_2^N	8.4386e-03	4.1114e-03	1.4553e-03	4.9621e-04	1.8232e-04
ρ_2^N	1.0374	1.4983	1.5523	1.4445	

Table 10. Uniform maximum error and its rate of convergence across the edge e_3 for solution component u_3 for Example 1(b) with $\varepsilon \in \mathbf{S}$.

N	64	128	256	512	1024
E_3^N	1.2070e-02	4.8465e-03	1.8153e-03	6.4873e-04	2.5092e-04
ρ_3^N	1.3164	1.4167	1.4845	1.3704	

Table 11. Uniform error and its rate of convergence overall solution components across the 3-star graphs throughout the discrete domain, for Example 1(b).

N	64	128	256	512	1024
E^N	1.2070e-02	4.8465e-03	1.8153e-03	6.4873e-04	2.5092e-04
ρ^N	1.3164	1.4167	1.4845	1.3704	

Table 12. Uniform maximum error and its rate of convergence across the whole domain for approximating solution component u_1 along edge e_1, for Example 1(c), with $\varepsilon \in \mathbf{S}$.

N	64	128	256	512	1024
E_1^N	2.7623e-01	7.9917e-02	2.0449e-02	5.6750e-03	1.7093e-03
ρ_1^N	1.7893	1.9665	1.8493	1.7312	

Table 13. Uniform maximum error and its rate of convergence across the edge e_2 for solution component u_2 for Example 1(c) with $\varepsilon \in \mathbf{S}$.

N	64	128	256	512	1024
E_2^N	8.3638e-01	1.1290e-01	2.6808e-02	7.2255e-03	2.0394e-03
ρ_2^N	2.8891	2.0743	1.8915	1.8250	

Table 14. Uniform maximum error and its rate of convergence across the edge e_3 for solution component u_3 for Example 1(c) with $\varepsilon \in \mathbf{S}$.

N	64	128	256	512	1024
E_3^N	5.4386e-01	1.4482e-01	3.9684e-02	1.1364e-02	3.4270e-03
ρ_3^N	1.9090	1.8677	1.8041	1.7294	

Table 15. Uniform error over all solution components across the 3-star graph and corresponding rate of convergence throughout the discrete domain, for Example 1(c).

N	64	128	256	512	1024
E^N	8.3638e-01	1.4482e-01	3.9684e-02	1.1364e-02	3.4270e-03
ρ^N	2.5299	1.8677	1.8041	1.7294	

The boundary and interior layers, along with their sharpness, are visible across all edges of the solution components, as shown in Figures 3a–5a for very small values of perturbation parameters. Additionally, Figures 3b–5b illustrate that the experimental rate of convergences match with the established theoretical rate of convergences over all edges of the 3-star graphs. Moreover, Figure 6 demonstrates that the solution components along the corresponding edges agree with the continuity condition (4.10).

Hence, we conclude that a suitable transformation of row entries of stiffness matrices (corresponding to the three-point scheme at interior and boundary points and the five-point scheme at the point of discontinuity) can lead to higher-order accurate solutions (compared to first order accurate solutions as available in [49]) for nonlinear reaction-dominated problems that are connected by the 3-star graph.

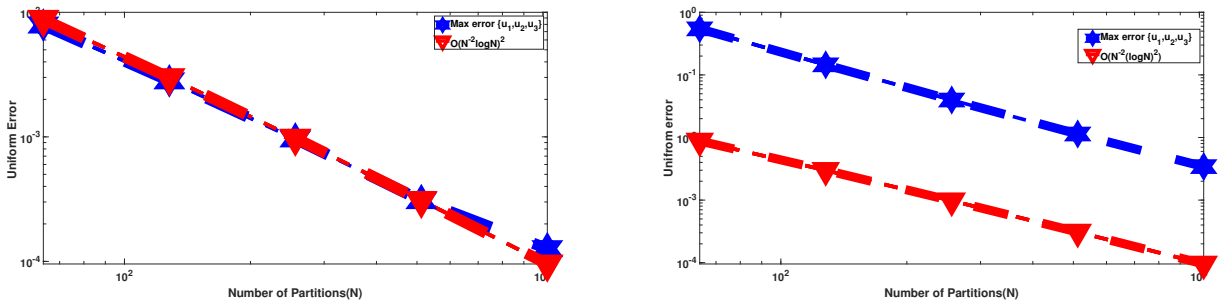

(a) Example 1(a). **(b)** Example 1(b).

Figure 3. Loglog plot of uniform errors overall solution components.

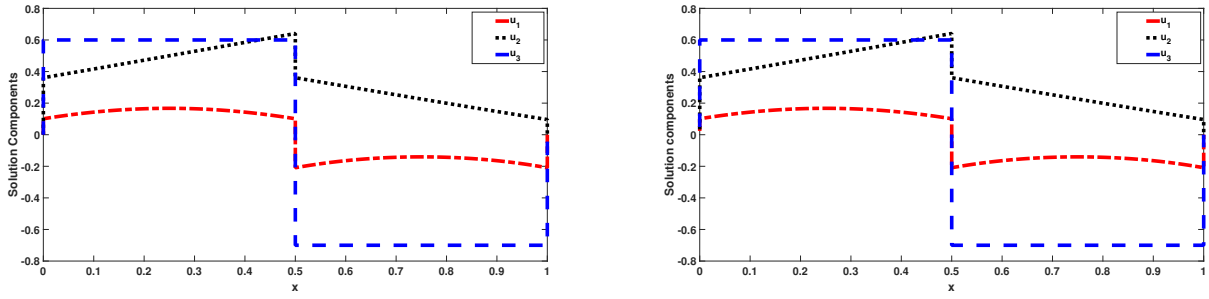

(a) Example 1(a). **(b)** Example 1(b).

Figure 4. Boundary and interior layers originated solution components with $N = 256$ and $\varepsilon_i = 2^{-40}$.

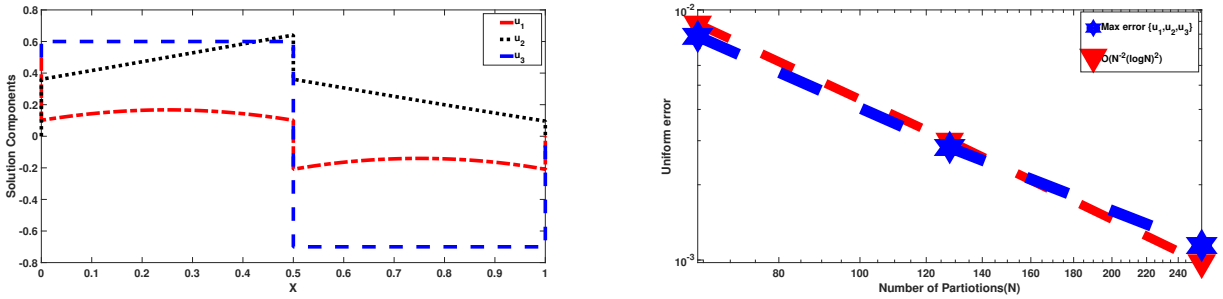

(a) Boundary and interior layers with $N = 256$ and $\varepsilon_i = 2^{-40}$. **(b)** Loglog plot of uniform errors.

Figure 5. Layers originated solution components and Loglog plot for Example 1(c).

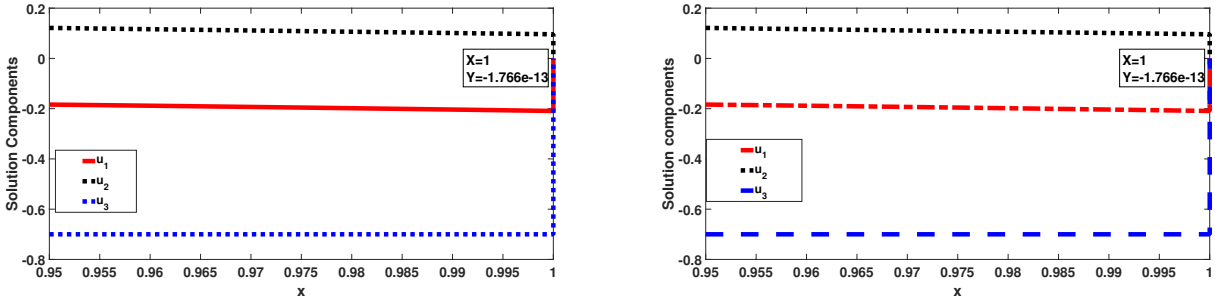

(a) Magnified version of Figure 3a . **(b)** Magnified version of Figure 5a.

Figure 6. A magnified view of the solution components near the right boundary is provided, here. This view clearly illustrates that each solution component adheres to the continuity condition (5.5) at the junction point $(1, 1.766e^{-13})$.

6. Conclusions

We examine a semi-linear singularly perturbed reaction-diffusion problem with non-smooth data on a k-star graph. Here, we consider all possible boundary conditions at the free boundary, specifically at the tail of the edge. At the junction point of the graph, we impose the natural and relevant requirements of continuity and Kirchhoff's junction law. Kirchhoff's junction law involves the first derivative at the junction point. Hence this makes the original problem coupled. First, we apply the flux condition at the free boundary, which is approximated by a first-order upwind approximation. To enhance this accuracy, we employ a three-point scheme for first-order derivatives and a central difference scheme for second-order derivatives. Generally, these approximations do not lead to an M-matrix or diagonal dominant structure of the stiffness matrix. Hence, we transform this scheme and establish sufficient conditions under which the stiffness matrix will be diagonally dominant. Additionally, we conduct a rigorous convergence analysis of this scheme, demonstrating almost second-order accuracy for each problem defined on the edges of the graph and for the coupled system defined on the star graph as well. Our numerical experiments further confirm the practical significance of our scheme, supported by experimental evidence. In the future, we aim to extend this work to a system of weakly and strongly coupled differential equations connected by more general graphs, such as cycles and complete graphs.

In these cases, the computational costs will be high and will be considered future goals.

Author contributions

All authors have contributed equally.

Use of AI tools declaration

The authors declare they have not used Artificial Intelligence (AI) tools in the creation of this article.

Conflict of interest

Higinio Ramos and Pratibhamoy Das are guest editors for Networks and Heterogeneous Media and was not involved in the editorial review or the decision to publish this article. All authors declare that there are no competing interests.

Acknowledgments

The author, Pratibhamoy Das, acknowledges the support of the Science and Engineering Research Board, Government of India, under Project No. MTR/2021/000797, which facilitated the completion of this work. This work was also supported by the University Grants Commission (UGC), India, through the Junior Research Fellowship (JRF) awarded to Dilip Sarkar, who gratefully acknowledges this support. The author, Shridhar Kumar, gratefully acknowledges the Indian Institute of Technology Patna for providing the institute fellowship.

References

1. Y. V. Pokornyi, A. V. Borovskikh, Differential equations on networks (geometric graphs), *J. Math. Sci.*, **119** (2004), 691–718. https://doi.org/10.1023/B:JOTH.0000012752.77290.fa
2. B. S. Pavlov, M. D. Faddeev, Model of free electrons and the scattering problem, *Theor. Math. Phys.*, **55** (1983), 485–492. https://doi.org/10.1007/BF01015809
3. T. Nagatani, Traffic flow on star graph: Nonlinear diffusion, *Physica A*, **561** (2021), 125251. https://doi.org/10.1016/j.physa.2020.125251
4. D. B. West, Introduction to graph theory, *Prentice Hall, Inc.*, Upper Saddle River, NJ, 1996.
5. W. C. Connor, J. Wengong, R. Luke, F. J. Timothy, S. J. Tommi, H. G. William, et al., A graph-convolutional neural network model for the prediction of chemical reactivity, *Chem. Sci.*, **10** (2019), 370–377. https://doi.org/10.1039/C8SC04228D
6. J. D. Murray, Mathematical biology: II: Spatial models and biomedical applications, *Interdiscip. Appl. Math.*, 2003.
7. L. O. Müller, G. Leugering, P. J. Blanco, Consistent treatment of viscoelastic effects at junctions in one-dimensional blood flow models, *J. Comput. Phys.*, **314** (2016), 167–193. https://doi.org/10.1016/j.jcp.2016.03.012

8. I. Rodriguez-Iturbe, R. Muneepeerakul, E. Bertuzzo, S. A. Levin, A. Rinaldo, River networks as ecological corridors: A complex systems perspective for integrating hydrologic, geomorphologic, and ecologic dynamics, *Water Resour. Res.*, **45** (2009), 1–22. https://doi.org/10.1029/2008WR007124

9. J. V. Below, A. J. Lubary, Instability of stationary solutions of reaction-diffusion equations on graphs, *Results Math.*, **68** (2015), 171–201. https://doi.org/10.1007/s00025-014-0429-8

10. S. Iwasaki, S. Jimbo, Y. Morita, Standing waves of reaction-diffusion equations on an unbounded graph with two vertices, *SIAM J. Appl. Math.*, **82** (2022), 1733–1763. https://doi.org/10.1137/21M1454572

11. H. M. Srivastava, A. K. Nain, R. K. Vats, P. Das, A theoretical study of the fractional-order p-Laplacian nonlinear Hadamard type turbulent flow models having the Ulam–Hyers stability, *Rev. Real Acad. Cienc. Exactas Fis. Nat. Ser. A-Mat.*, **117** (2023), 1–19. https://doi.org/10.1007/s13398-023-01488-6

12. V. Mehandiratta, M. Mehra, G. Leugering, Existence and uniqueness results for a nonlinear Caputo fractional boundary value problem on a star graph, *J. Math. Anal. Appl.*, **477** (2019), 1243–1264. https://doi.org/10.1016/j.jmaa.2019.05.011

13. D. G. Gordeziani, M. Kupreishvili, H. V. Meladze, T. D. Davitashvili, On the solution of boundary value problem for differential equations given in graphs, *Appl. Math. Inform. Mech.*, **13** (2008), 80–91.

14. G. M. Gie, M. Hamouda, C. Y. Jung, R. M. Temam, *Singular Perturbations and Boundary Layers*, Springer International Publishing, 2018. https://doi.org/10.1007/978-3-030-00638-9

15. P. Das, S. Rana, J. Vigo-Aguiar, Higher-order accurate approximations on equidistributed meshes for boundary layer originated mixed type reaction-diffusion systems with multiple scale nature, *Appl. Numer. Math.*, **148** (2020), 79–97. https://doi.org/10.1016/j.apnum.2019.08.028

16. P. Das, Comparison of a priori and a posteriori meshes for singularly perturbed nonlinear parameterized problems, *J. Comput. Appl. Math.*, **290** (2015), 16–25. https://doi.org/10.1016/j.cam.2015.04.034

17. P. Das, An a posteriori based convergence analysis for a nonlinear singularly perturbed system of delay differential equations on an adaptive mesh, *Numerical Algorithms*, **81** (2019), 465–487. https://doi.org/10.1007/s11075-018-0557-4

18. P. Das, A higher order difference method for singularly perturbed parabolic partial differential equations, *J. Differ. Equations Appl.*, **24** (2018), 452–477. https://www.tandfonline.com/doi/full/10.1080/10236198.2017.1420792

19. D. Shakti, J. Mohapatra, P. Das, J. Vigo-Aguiar, A moving mesh refinement based optimal accurate uniformly convergent computational method for a parabolic system of boundary layer originated reaction-diffusion problems with arbitrary small diffusion terms, *J. Comput. Appl. Math.*, **404** (2022), 113167. https://doi.org/10.1016/j.cam.2020.113167

20. S. Kumar, P. Das, K. Kumar, Adaptive mesh-based efficient approximations for Darcy scale precipitation–dissolution models in porous media, *Int. J. Numer. Methods Fluids*, **96** (2024), 1415–1444. https://doi.org/10.1002/fld.5294

21. S. Saini, P. Das, S. Kumar, Parameter uniform higher order numerical treatment for singularly perturbed Robin type parabolic reaction-diffusion multiple scale problems with large delay in time, *Appl. Numer. Math.*, **196** (2024), 1–21. https://doi.org/10.1016/j.apnum.2023.10.003
22. S. Sain, P. Das, S. Kumar, Computational cost reduction for coupled system of multiple scale reaction-diffusion problems with mixed type boundary conditions having boundary layers, *Rev. Real Acad. Cienc. Exactas Fís. Nat. Ser. A Mat.*, **117** (2023), 1–27. https://doi.org/10.1007/s13398-023-01397-8
23. S. Kumar, P. Das, A uniformly convergent analysis for multiple scale parabolic singularly perturbed convection-diffusion coupled systems: Optimal accuracy with less computational time, *Appl. Numer. Math.*, **207** (2025), 534–557. https://doi.org/10.1016/j.apnum.2024.09.020
24. B. P. Andreianov, G. M. Coclite, C. Donadello, Well-posedness for vanishing viscosity solutions of scalar conservation laws on a network, *Discrete Contin. Dyn. Syst.*, **37** (2017), 5913–5942. http://dx.doi.org/10.3934/dcds.2017257
25. M. Musch, U. S. Fjordholm, N. H. Risebro, Well-posedness theory for nonlinear scalar conservation laws on networks, *Networks Heterogen. Media*, **17** (2022), 101–128. https://doi.org/10.3934/nhm.2021025
26. G. M. Coclite, C. Donadello, Vanishing viscosity on a star-shaped graph under general transmission conditions at the node, *Networks Heterogen. Media*, **15** (2020), 197–213. https://doi.org/10.3934/nhm.2020009
27. J. D. Towers, An explicit finite volume algorithm for vanishing viscosity solutions on a network, *Networks Heterogen. Media*, **17** (2022), 1–13. https://doi.org/10.3934/nhm.2021021
28. S. F. Pellegrino, On the implementation of a finite volumes scheme with monotone transmission conditions for scalar conservation laws on a star-shaped network, *Appl. Numer. Math.*, **155** (2020), 181–191. https://doi.org/10.1016/j.apnum.2019.09.011
29. F. R. Guarguaglini, R. Natalini, Vanishing viscosity approximation for linear transport equations on finite star-shaped networks, *J. Evol. Equations*, **21** (2021), 2413–2447. https://doi.org/10.1007/s00028-021-00688-0
30. H. Egger, N. Philippi, On the transport limit of singularly perturbed convection-diffusion problems on networks, *Math. Methods Appl. Sci.*, **44** (2021), 5005–5020. https://doi.org/10.1002/mma.7084
31. H. Egger, N. Philippi, A hybrid discontinuous Galerkin method for transport equations on networks, in *Finite volumes for complex applications IX*, Bergen, Norway, Springer, **323** (2020), 487–495. https://doi.org/10.1007/978-3-030-43651-3_45
32. H. Egger, N. Philippi, A hybrid-DG method for singularly perturbed convection-diffusion equations on pipe networks, *ESAIM Math. Model. Numer. Anal.*, **57** (2023), 2077–2095. https://doi.org/10.1051/m2an/2023044
33. V. Kumar, G. Leugering, Singularly perturbed reaction-diffusion problems on a k-star graph, *Math. Methods Appl. Sci.*, **44** (2021), 14874–14891. https://doi.org/10.1002/mma.7749

34. P. A. Farrell, J. J. H. Miller, E. O'Riordan, G. I. Shishkin, Singularly perturbed differential equations with discontinuous source terms, in *Analytical and Numerical Methods for Convection-Dominated and Singularly Perturbed Problems* (eds. J.J.H. Miller, G.I. Shishkin and L. Vulkov), Nova Science Publishers, New York, (2000), 23–32.

35. Z. Cen, A hybrid difference scheme for a singularly perturbed convection-diffusion problem with discontinuous convection coefficient, *Appl. Math. Comput.*, **169** (2005), 689–699. https://doi.org/10.1016/j.amc.2004.08.051

36. S. Kumar, S. Kumar, P. Das, Second-order a priori and a posteriori error estimations for integral boundary value problems of nonlinear singularly perturbed parameterized form, *Numerical Algorithms*, 2024. https://doi.org/10.1007/s11075-024-01918-5

37. S. Santra, J. Mohapatra, P. Das, D. Choudhari, Higher-order approximations for fractional order integro-parabolic partial differential equations on an adaptive mesh with error analysis, *Comput. Math. Appl.*, **150** (2023), 87–101. https://doi.org/10.1016/j.camwa.2023.09.008

38. V. Kumar, G. Leugering, Convection dominated singularly perturbed problems on a metric graph, *J. Comput. Appl. Math.* **425** (2023), 115062. https://doi.org/10.1016/j.cam.2023.115062

39. H. Zhu, Z. Li, Z. Yang, Analysis and computation for a class of semilinear elliptic boundary value problems, *Comput. Math. Appl.*, **64** (2012), 2735–2743. https://doi.org/10.1016/j.camwa.2012.08.004

40. J. J. Nieto, J. M. Uzal, Nonlinear second-order impulsive differential problems with dependence on the derivative via variational structure, *J. Fixed Point Theory Appl.*, **22** (2020), 1–19. https://doi.org/10.1007/s11784-019-0754-3

41. K. Atkinson, W. Han, *Theoretical Numerical Analysis: A Functional Analysis Framework*, Springer, New York, 2009.

42. G. V. Alekseev, R. V. Brizitskii, Z. Y. Saritskaya, Stability estimates of solutions to extremal problems for a nonlinear convection-diffusion-reaction equation, *J. Appl. Ind. Math.*, **10** (2016), 155–167. https://doi.org/10.17377/sibjim.2016.19.201

43. M. Manikandan, R. Ishwariya, Robust computational technique for a class of singularly perturbed nonlinear differential equations with Robin boundary conditions, *J. Math. Model.*, **11** (2023), 411–423. https://doi.org/10.22124/jmm.2023.23515.2100

44. R. Shiromani, V. Shanthi, P. Das, A higher order hybrid-numerical approximation for a class of singularly perturbed two-dimensional convection-diffusion elliptic problem with non-smooth convection and source terms, *Comput. Math. Appl.*, **142** (2023), 9–30. https://doi.org/10.1016/j.camwa.2023.04.004

45. M. Chandru, T. Prabha, V. Shanthi, A hybrid difference scheme for a second-order singularly perturbed reaction-diffusion problem with non-smooth data, *Int. J. Appl. Comput. Math.*, **1** (2015), 87–100. https://doi.org/10.1007/s40819-014-0004-8

46. J. J. H. Miller, E. O'Riordan, G. I. Shishkin, *Fitted Numerical Methods for Singular Perturbation Problems: Error Estimates in the Maximum Norm for Linear Problems in One and Two Dimensions*, World Scientific, 1996.

47. P. A. Farrell, A. F. Hegarty, J. J. H. Miller, E. O'Riordan, G. I. Shishkin, *Robust Computational Techniques for Boundary Layers*, Chapman and Hall, CRC Press, Boca Raton, USA, 2000.
48. N. Kopteva, M. Stynes, Numerical analysis of a singularly perturbed nonlinear reaction-diffusion problem with multiple solutions, *Appl. Numer. Math.*, **51** (2004), 273–288. https://doi.org/10.1016/j.apnum.2004.07.001
49. S. Kumar, R. Ishwariya, P. Das, Impact of mixed boundary conditions and non-smooth data on layer originated non-premixed combustion problems: Higher order convergence analysis, *Stud. Appl. Math.*, (2024), e12673. https://doi.org/10.1111/sapm.12763

AIMS Press